Infectious subgenomic amplicon strategies for Japanese encephalitis and West Nile viruses

Prince Pal Singh[1,2], Nguyen Phuong Khanh Le[1], Uladzimir Karniychuk[1,*]

[1]Department of Veterinary Biosciences, College of Veterinary Medicine, The Ohio State University, Columbus, OH, USA

[2]School of Public Health, University of Saskatchewan, Saskatoon, Canada

***Correspondence:** Uladzimir Karniychuk

Department of Veterinary Biosciences, College of Veterinary Medicine, The Ohio State University, Columbus, OH, USA

karniychuk.1@osu.edu

ABSTRACT

Classical methods for constructing infectious cDNA clones of flaviviruses are often hindered by instability and toxicity. The Infectious-Subgenomic-Amplicons (ISA) method is an advancement which utilizes overlapping DNA fragments representing viral genomic sequence and in-cell recombination to bypass bacterial plasmid assembly. However, the ISA method has limitations due to the toxicity of some ISA DNA fragments in bacteria during synthetic production. We validated modified ISA strategies for producing toxic ISA Japanese encephalitis virus (JEV) and West Nile virus (WNV) DNA fragments. Three approaches were explored including subdividing toxic DNA fragments into two sub-fragments for synthetic clonal production, using a low-copy bacterial plasmid, and subdividing the toxic DNA fragments into four short overlapping sub-fragments, each up to 1.8 kb. The latter novel approach in ISA applications enabled the synthesis of entirely bacteria-free ISA DNA fragments. Our results demonstrate that subdividing toxic fragments into sub-fragments smaller than 1.8 kb for synthesis is the efficient strategy, circumventing the need for bacterial plasmids and ensuring rapid production of synthetic flaviviruses. This method also shortens the production timeline. We also compared the efficacy of JEV and WNV ISA in zinc finger antiviral protein 1 (ZAP) wild-type and knockout cells and found that knockout cells may be more effective for ISA rescue of flaviviruses, including attenuated strains for live attenuated vaccines. The validated modified ISA strategies provide an efficient approach for producing synthetic JEV and WNV. This will enable rapid research during outbreaks of emerging flaviviruses by facilitating the quick generation of new virus variants.

Flavivirus, Japanese encephalitis virus, West Nile virus, dengue virus, infectious subgenomic amplicons, ZAP, reverse genetics, infectious clones

INTRODUCTION

Flaviviruses are single-stranded RNA viruses transmitted mainly by arthropods, as well as sexually and transplacentally. The genus Flavivirus (family *Flaviviridae*) comprises viruses which cause human disease, including dengue virus (DENV), Japanese encephalitis virus (JEV), and West Nile virus (WNV). These flaviviruses infect millions of people each year, causing symptoms from mild fevers to fatal hemorrhagic and neurological diseases [1]. The rising number of global flavivirus infections, frequent outbreaks, and expanding geographical range pose significant public health concerns [1]. Flaviviruses also pose constant threats to livestock industries [2]. There are no approved human vaccines for certain flaviviruses, such as Zika virus and WNV. Moreover, no licensed antivirals exist against flaviviruses.

There are four DENV serotypes which cause illnesses ranging from mild dengue fever to severe life-threatening dengue. Dengue virus is the major cause of hospitalization and death in children in Southeast Asian countries. Annually, DENV results in approximately 390 million infections, 100 million clinically apparent cases, and 500,000 severe cases, with at least 2.5 billion people at risk [1,3]. Over the past 70 years, infection rates have steadily increased, making DENV the most prevalent arthropod-borne viral disease worldwide. By comparison, only sporadic DENV epidemics were documented before the Second World War [1,4]. Between 2010 and 2022, more than 33,000 locally acquired dengue cases have been reported in the USA. Since 2014, there have been fewer than 1,000 cases per year, but 2022 was the first time in a decade that cases reached four digits. In 2023, Florida officials issued a warning about dengue as the cases continued to increase.

Japanese encephalitis virus causes encephalitis in humans in the Asia-Pacific region [5], with 68,000 annual cases and 15,000 deaths [6]. JEV epidemics were originally described in Japan in the 19th century, and the virus was first recovered in 1935 from an infected human in Tokyo [1]. The enzootic cycle of JEV is between water birds and *Culex* mosquitoes, with pigs also serving as an amplifying host [1]. Humans are considered incidental dead-end hosts and generally do not produce viremia sufficient to infect mosquitoes. Though many human infections are asymptomatic, around 20-30% of clinical infections are fatal, and 30-50% of the survivors develop life-long neurological sequelae [5]. Human transplacental and fetal JEV infections are also reported [7]. The geographic range of emerging JEV keeps expanding from the South of Russia to Australia, Japan, Eastern China, India, and South-East Asia. Also, severe travel-related cases are reported around the globe [8]. There is a concern that JEV can be introduced into North America given a large population of susceptible avian species and amplifying hosts—pigs, wild boars; susceptible *Culex* mosquitoes are also ubiquitous [9-11]. In addition to morbidity and mortality in humans, JEV causes economically significant clinical disease in pigs, mostly abortions and stillbirth [11,12]. Japanese encephalitis virus keeps expanding—the 2022 JEV outbreak in Australia with infections in swine herds, zoonotic transmission, and human deaths was caused by genotype IV which was not associated with outbreaks before [13].

West Nile virus (WNV) is classified by the National Institute of Allergy and Infectious Diseases as a "Category B Priority" pathogen, indicating its high threat level. West Nile virus cycles between *Culex* mosquitoes and birds, but it can also infect humans, horses, and other mammals. The virus is widespread, found in Africa, the Middle East, West Asia, Australia, the Americas, and Europe. The first major European outbreak occurred in Romania in 1996, with the largest in

2018 affecting 12 countries. In the U.S., WNV emerged in 1999, rapidly spreading and causing significant morbidity and annual outbreaks, notably in 2002, 2003, and 2012 [1,14].

West Nile virus is neuroinvasive, leading to central nervous system damage, including meningitis and encephalitis, which can be fatal or cause long-term disabilities such as a poliomyelitis-like syndrome. The virus's spread has increased due to expanding mosquito habitats and changing bird migration patterns caused by climate change. Currently, it is the most common insect-borne zoonotic virus in the U.S., with no approved human vaccines or antivirals. From 1999 to 2010, blood supply screening estimated 2 to 4 million total infections in the U.S. [15]. In 2022, Centers for Disease Control and Prevention reported 1,126 cases and 93 deaths in the U.S., and 2,406 cases and 1,599 neuroinvasive diseases in 2023, underscoring growing cases and inadequate environmental controls.

Reverse genetics, defined as the generation of viruses entirely from complementary DNA (cDNA) [16], has revolutionized virology research, including research of flaviviruses. This powerful technique enables the experimental editing of viral genomes to investigate effects of point mutations, host-pathogen interactions, virulence factors, mechanisms of immune evasion, and the development of reporter viruses, vaccines, and antiviral testing [17,18]. The classical method involves constructing an infectious DNA clone. This clone is typically a bacterial DNA plasmid or two plasmids containing the entire cDNA of the viral genome and a suitable promoter, such as the T7 promoter [17,19]. In this approach, viral RNA is obtained from biological specimens, and a double-stranded cDNA copy of the RNA virus genome is generated and incorporated into plasmids, which are then amplified in bacteria. After plasmid purification,

115 infectious viruses are produced either by direct transfection of permissive cells or by transfection
116 of genomic RNA obtained through *in vitro* transcription [17,19].
117
118 Despite advances in molecular techniques, classical methods for constructing infectious cDNA
119 clones are time-consuming, unpredictable, and labor-intensive and frequently associated with
120 undesirable mutations or unstable and toxic clones in bacteria [17,19]. Flavivirus infectious DNA
121 clones are particularly challenging due to the instability and toxicity of some viral sequences in
122 bacterial hosts [17-23]. To mitigate these difficulties, bacteria-free approaches have been
123 developed, including long PCR, circular polymerase extension reaction, Gibson assembly, and
124 Infectious-Subgenomic-Amplicons (ISA) [17].
125
126 The ISA method represents a significant advancement in reverse genetics for flaviviruses [24]. It
127 allows to bypass the problematic step of assembling and amplifying the full-length flavivirus
128 genome in bacterial plasmids and bacterial cells. Instead, the ISA process relies on in-cell
129 recombination, which simplifies and shortens the procedure where overlapping PCR-amplified
130 ISA DNA fragments, flanked with a pCMV promoter and HDR/SV40pA sequences, are directly
131 transfected into mammalian cells, insect cells, or *in vivo* in mice [17,25]. For example, in the
132 most recent study using the classical ISA the authors rescued DENV; in contrast cloning the full-
133 length DENV genome in bacteria failed due to toxicity [19].
134
135 While ISA is termed a "bacteria-free" approach, it is not completely free of bacteria and
136 associated toxicity issues. Specifically, to our knowledge all sixteen published studies utilizing
137 ISA for flavivirus rescue have used PCR amplification of fragments from pre-existing full-length

138 flavivirus DNA infectious clones, infected biological specimens, or synthetic overlapping DNA
139 ISA fragments. These later synthetic DNA fragments, provided by commercial suppliers, are
140 assembled, inserted into bacterial plasmids, and amplified in bacteria [19,24-38]. Although this
141 approach avoids constructing unstable and toxic plasmids containing sequences of the entire viral
142 genome, some synthetic ISA DNA fragments still may pose bacterial toxicity, slowing or halting
143 their commercial production. Indeed, in several of these papers, along with commercially
144 generated ISA DNA fragments, the authors PCR-amplified some ISA DNA fragments directly
145 from historically preexisting entire-genome-length flavivirus infectious DNA clones or from
146 infected biological specimens to rescue yellow fever virus, DENV, and JEV [24,34]. While the
147 reason for applying this mixed, not entirely synthetic reverse genetics approach was not
148 explicitly explained in these publications, it is likely due to the toxicity of ISA DNA fragments
149 preventing commercial generation of fragments for fully synthetic flaviviruses.
150
151 In our studies, we encountered similar technical difficulties with the toxicity of flavivirus ISA
152 DNA fragments, which impeded commercial suppliers' ability to provide the required fragments.
153 Given the importance of generating entirely synthetic flavivirus stocks for certain experimental
154 objectives, in this study we applied and validated modified ISA strategies. These approaches
155 allowed us to generate JEV and WNV using a completely synthetic method for toxic ISA
156 flavivirus fragments.
157
158 **MATERIALS AND METHODS**
159 Wild-type and CCCH-type zinc finger antiviral protein (ZAP) knockout cells, *in silico*
160 permutation of the viral genome, ISA, DENV, JEV, and WNV stock generation and titration,

161 comparative ISA, mouse experiments, RT-qPCR, and statistics are described in supplemental
162 materials and methods.
163
164 **RESULTS**

165 **Classical Infectious-Subgenomic-Amplicons method for dengue virus**

166 As described before [19], transfection of three overlapping ISA DNA fragments generated via
167 *synthetic clonal genes* with medium copy number bacterial plasmids (**Table S1**) and
168 amplification in bacteria (**Fig 1**) consistently rescued infectious DENV in all five well replicates.
169 The virus induced a cytopathic effect (CPE) in all transfected wells at passages 0 and 1 (**Fig 2A**),
170 as well as in flasks during subsequent passaging and virus stock generation. Sanger sequencing
171 confirmed correct sequences in the DENV stock. The DENV stock produced in VERO-ZAP-KO
172 cells exhibited high infectious titers when titrated on both VERO-ZAP-WT and VERO-ZAP-KO
173 cells (**Fig 2B**), along with high viral RNA loads (**Fig 2C**) and E protein expression (**Fig 2D**).
174
175 Altogether, as in the previous study [19], we confirmed that classical ISA (**Fig 1**) with three
176 overlapping DNA fragments generated via *synthetic clonal genes* with bacterial plasmids is a
177 highly efficient and robust technique for type 2 DENV reverse genetics, enabling the rescue of
178 synthetic recombinant viruses. The properties of ISA-derived DENV have been extensively
179 characterized in prior research [19]; thus, we further focused on the more challenging ISA
180 strategies for JEV and WNV.
181

182 **Infectious-Subgenomic-Amplicons method to overcome bacterial toxicity caused by**

183 **Japanese encephalitis virus sequences**

184 In contrast to DENV, classical ISA failed to rescue the JEV SA14-14-2 wild-type strain (JEV-
185 WT). The JEV Fragment I exhibited bacterial toxicity across three different medium and low
186 copy bacterial plasmids (**Table S1, Fig 3**). To overcome this, we divided the toxic Fragment I
187 sequence (4,550 bp) into two sub-fragments, Fragment-I-A and Fragment-I-B, each 2,315-2,316
188 bp. These sub-fragments were produced via *synthetic clonal genes* using medium copy number
189 bacterial plasmids and amplified in bacteria (**Table S1, Fig 3, File S1**). Transfection of four
190 overlapping ISA DNA fragments generated via *synthetic clonal genes* (**Fig 3**) consistently
191 rescued infectious JEV-WT in all five replicates. The virus induced CPE in all transfected wells
192 at passages 0 and 1 (**Fig 4A**), as well as in flasks during subsequent passaging and virus stock
193 generation. Sanger sequencing confirmed correct sequences in the JEV-WT stock. The JEV-WT
194 stock produced in VERO-ZAP-KO cells exhibited high infectious titers when titrated on both
195 VERO-ZAP-WT and VERO-ZAP-KO cells (**Fig 4B**), along with high viral RNA loads (**Fig 4B**)
196 and E protein expression (**Fig 4C**).

197

198 Enrichment of CpG dinucleotides in viral genomes is an emerging approach for live attenuated
199 vaccines and oncolytics [26-29,39]. We generated CpG-enriched JEV (JEV-CpG) (**Table S1**,
200 **Table S2**, **File S2**) using the same ISA strategy as for JEV-WT (**Fig 3**). The Fragment I
201 sequence was subdivided into two sub-fragments, Fragment-I-A and Fragment-I-B, produced
202 using *synthetic clonal genes* in medium copy number bacterial plasmids. Transfection of four
203 overlapping ISA DNA fragments successfully rescued infectious JEV-CpG in all five replicates,

204 with the virus inducing CPE in all transfected wells at passages 0 and 1 (**Fig 4D**). Sanger
205 sequencing confirmed the correct sequences in the JEV-CpG stock. The JEV-CpG stock
206 produced in VERO-ZAP-KO cells showed high infectious titers on both VERO-ZAP-WT and
207 VERO-ZAP-KO cells (**Fig 4E**), along with high viral RNA loads (**Fig 4E**) and E protein
208 expression (**Fig 4G**). Consistent with previous enrichment studies in Zika virus [27,28], the
209 CpG-enriched JEV variant exhibited an attenuated phenotype in VERO-ZAP-WT cells (**Fig 4F**).

210

211 Next, we conducted a mouse study to identify whether JEV-WT and JEV-CpG obtained with the
212 synthetic ISA approach causes typical infection phenotypes *in vivo*. The SA14-14-2 JEV strain
213 does not cause infection in conventional mice; thus, we used *Ifnar1*$^{-/-}$ mice deficient for the type I
214 IFN receptor function. The wild SA14-14-2 JEV strain causes clinical signs and lethality in
215 *Ifnar1*$^{-/-}$ mice [40]. Five-week-old mice, six mice per group, were injected subcutaneously with
216 virus-free media (MOCK) or ISA-derived JEV-WT or JEV-CpG. Mice in the MOCK group did
217 not show clinical signs (**Fig 4H**); one MOCK mouse lost weight after manipulation and injection
218 but recovered. Mice in the JEV-WT group showed a high 50% mortality due to paralysis and loss
219 of 20% baseline body weight (**Fig 4H**). Another 50% of mice in the JEV-WT group also showed
220 clinical signs—ataxia, depression and hunching but survived. Consistent with previous
221 enrichment studies in Zika virus [27,28], the JEV-CpG variant showed an attenuated phenotype
222 with no mortality or disease in mice (**Fig 4H**).

223

224 We tested spleen and brain from MOCK and JEV groups with the virus-specific RT-qPCR assay.
225 As expected, JEV RNA was not detected in the MOCK group (**Fig 4I**). All samples from the
226 JEV-WT group showed high viral RNA loads—$10^{5.58-7.52}$ RNA copies per g of the brain, and

227 $10^{5.44-7.60}$ RNA copies per g of the spleen (**Fig 4I**). In contrast, all brain samples from the JEV-
228 CpG group were negative in RT-qPCR (**Fig 4I**). JEV-CpG RNA loads in the spleen were
229 considerably lower ($P < 0.0001$, t-test) than JEV-WT loads (**Fig 4I**).
230
231 Infection phenotypes in our study with the ISA-derived JEV-WT were comparable to the
232 infection phenotypes in the previous study where *Ifnar1*$^{-/-}$ mice injected with the wild (not
233 synthetic) SA14-14-2 JEV strain also showed mortality, clinical signs, and virus in the spleen
234 [40]. In contrast to our study however, the authors did not find wild SA14-14-2 JEV in the brain.
235 The discrepancy can be explained by the different sampling time—at 12 days after injection in
236 our study, and 4 days in the previous study [40]. Also, in the previous study, mice injected with
237 $10^{6.7}$ plaque forming units (PFU) showed 100% mortality, while mice in our study
238 (10^7 $TCID_{50}$/mouse) showed 50% mortality and 100% morbidity. The difference may be due to
239 different methods to quantify viral loads for injection (PFU versus $TCID_{50}$ assay), the route of
240 injection—intraperitoneal previously and subcutaneous in our study, and potentially reduced
241 viral population complexity in synthetically rescued JEV compared to wild viruses.
242
243 Altogether, dividing the toxic JEV fragment into two sub-fragments provides a highly efficient
244 and robust ISA approach for reverse genetics. This method overcomes the bacterial toxicity
245 caused by JEV sequences and enables the successful rescue of synthetic recombinant JEV.
246
247

248 **Infectious-Subgenomic-Amplicons methods to overcome bacterial toxicity caused by West**
249 **Nile virus sequences**

250 During the rescue of the wild-type WNV NY99 strain (WNV-WT), Fragment I exhibited
251 bacterial toxicity when using a medium copy bacterial plasmid (**Fig 5**). To address this, a low
252 copy plasmid was utilized (**Fig 5**), which enabled the successful rescue of Fragment I after
253 several attempts over a three-month period.

254

255 As observed with JEV (**Fig 3**), classical ISA failed to rescue the WNV NY99 strain which was
256 permutated (WNV-Per) to generate the permutated control virus (see materials and methods; **File**
257 **S2**, **Table S2**) across three different medium and low copy bacterial plasmids (**Table S1, Fig 6**).
258 To overcome this issue, the toxic Fragment I sequence (4,358 bp) was divided into three sub-
259 fragments: Fragment-I-A (1,198 bp), Fragment-I-B (1,126 bp), and Fragment-I-c (2,179 bp)
260 (**Table S1, File S1**). The first two fragments were made shorter to facilitate bacteria-free
261 *synthesis of DNA* (available only for fragments shorter than 1.8 kb) based on the assumption that
262 the 5' flanking CMV promoter sequence contributed to the toxicity in bacteria. The longer
263 Fragment-I-c was used for *synthetic clonal genes* with medium copy plasmid and bacterial
264 amplification (**Table S1, File S1**). However, due to continued toxicity and failure, Fragment-I-c
265 was further subdivided into overlapping Fragment-I-C (1,162 bp) and Fragment-I-D (1,089 bp),
266 both small enough for bacteria-free *synthesis of DNA*. This troubleshooting led to the six
267 overlapping ISA fragments for WNV-Per (**Fig 6, Table S1, File S1**).

268

269 Transfection of the three overlapping ISA DNA fragments for WNV-WT and six overlapping
270 ISA DNA fragments for WNV-Per consistently rescued the corresponding infectious WNV
271 variants in all five replicates. Sanger sequencing confirmed correct sequences in WNV stocks.
272 Viruses induced CPE in all transfected wells at passages 0 and 1 (**Fig 7A, B**), as well as in flasks
273 during subsequent passaging and virus stock generation. Both WNV-WT and WNV-Per stocks
274 produced in VERO-ZAP-KO cells had high infectious titers when titrated on both VERO-ZAP-
275 WT and VERO-ZAP-KO cells (**Fig 7C, D**), along with high viral RNA loads (**Fig 7C, D**) and E
276 protein expression (**Fig 7E, F**).
277
278 Next, we conducted a mouse study to identify whether WNV-WT and WNV-Per variants
279 obtained with the synthetic ISA approach cause typical infection phenotypes *in vivo*. We used a
280 well-established C57BL/6J mouse model for severe WNV infection [41-43]. Six-week-old
281 C57BL/6J mice (14 mice per group) were MOCK infected or injected intraperitoneally (IP) with
282 WNV-WT or WNV-Per variants. Mice in the MOCK group did not show clinical signs, weight
283 loss, or mortality (**Fig 7G**). Mice in the WNV-WT and WNV-Per groups showed high
284 mortality—93% and 79% (**Fig 7G**), ataxia, depression, paralysis, loss of 20% body weight, and
285 death.
286
287 We tested spleen and brain from MOCK and WNV groups with the virus-specific RT-qPCR
288 assay. As expected, WNV RNA was not detected in the MOCK group (**Fig 7H**). In contrast, all
289 samples from the WNV-WT and WNV-Per groups showed high WNV RNA loads—$10^{4.98-6.97}$
290 RNA copies per g of the spleen, and $10^{5.78-8.72}$ RNA copies per g of the brain (**Fig 7H**). The
291 difference in viral RNA loads between WNV-WT and WNV-Per groups was not statistically

292 significant ($P < 0.05$), which is expected because permutation in the WNV-Per variant does not
293 affect encoded proteins and does not considerably affect genome coding parameters (**Table S2**).
294
295 Infection phenotypes in our study with the ISA-derived WNV variants were comparable to the
296 infection phenotypes in the previous study where C57BL/6J mice injected with the wild (not
297 synthetic) WNV NY99 strain also showed mortality, clinical signs, and virus in the spleen and
298 brain [41-43].
299
300 **Comparative Infectious-Subgenomic-Amplicons in ZAP wild-type and ZAP knockout cells**
301 The zinc finger antiviral protein 1 (ZAP) exhibits broad-spectrum antiviral activity. Recent
302 studies, including our own, have demonstrated that flaviviruses such as Zika virus, JEV, and
303 WNV are susceptible to ZAP antiviral effects in VERO cells [44-46]. Here, we compared the
304 efficiency of JEV and WNV ISA in wild-type (VERO-ZAP-WT) and ZAP knockout (VERO-
305 ZAP-KO) cells. We selected JEV-WT, JEV-CpG, and WNV-Per variants, using four and six ISA
306 fragments (**Figs 3, 6**) for comparative ISA. Infectious-Subgenomic-Amplicons for each variant
307 were performed concurrently, as described in the supplemental materials and methods, with DNA
308 amplicons for transfection into VERO-ZAP-WT or VERO-ZAP-KO cells derived from the same
309 PCR reactions.
310
311 JEV-WT induced CPE in all five replicates of both ZAP-WT and ZAP-KO cells during passage
312 0, with more pronounced CPE in ZAP-KO cells (**Fig 8A**). JEV-CpG also induced CPE in all five
313 replicates of both ZAP-WT and ZAP-KO cells during passage 0, with more pronounced CPE in
314 ZAP-KO cells (**Fig 8A**). WNV-Per caused equally strong CPE in both ZAP-WT and ZAP-KO

315 cells (**Fig 8A**). During passage 1, JEV-WT, JEV-CpG, and WNV-Per infections in ZAP-KO cells
316 were associated with higher E protein expression compared to ZAP-WT cells (***$P < 0.0001$;
317 **Figs 8B, D, F**). Consequently, JEV-CpG and WNV-Per $TCID_{50}$ infectious titers in supernatants
318 were significantly higher in ZAP-KO cells than in ZAP-WT cells ($P = 0.014$-0.017) (**Figs 8C, E,**
319 **J**).
320
321 Overall, both wild-type and ZAP knockout cells demonstrated 100% ISA efficiency, successfully
322 rescuing JEV and WNV in all five replicates. However, ISA in ZAP-KO cells resulted in the
323 considerably higher number of virus-positive cells and elevated infectious virus loads.
324

325 **DISCUSSION**

326 The goal of this study was to validate modified ISA strategies for producing toxic ISA flavivirus
327 DNA fragments synthetically, overcoming bacterial toxicity and eliminating the need to amplify
328 toxic fragments from biological specimens or other preexisting sources. These ISA strategies
329 enable the generation of entirely synthetic JEV and WNV stocks. The strategies involved: (i)
330 Subdividing the problematic toxic DNA fragment into two sub-fragments for subsequent
331 *synthetic clonal gene* production with bacterial plasmids and bacteria. (ii) Using a low copy
332 bacterial plasmid. (iii) Subdividing the toxic DNA fragment into four short overlapping sub-
333 fragments, each up to 1.8 kb, for subsequent bacteria-free *synthesis of DNA* production. To our
334 knowledge, the latter strategy had never been applied for ISA.
335
336 As expected, and previously demonstrated for the DENV 2 serotype [19], the classical ISA
337 approach of subdividing the flavivirus genome into three overlapping fragments of

338 approximately 4 kb each works well for DENV. These fragments were synthesized quickly and
339 without technical difficulties by a commercial supplier using a medium copy bacterial plasmid
340 (**Table S1**).
341 In contrast, this classical three-fragment ISA approach failed when we attempted to rescue JEV-
342 WT Fragment I using three different medium and low copy bacterial plasmids (**Table S1**). The
343 solution was to divide the toxic fragment into two sub-fragments. We encountered similar
344 technical difficulties producing WNV-WT Fragment I. Here, replacing the medium copy plasmid
345 with a low copy plasmid resolved the issue, allowing the rescue of the entirely synthetic WNV-
346 WT variant, but this took several attempts and over three months.
347 More challenging difficulties arose when we attempted to rescue the permuted WNV-Per variant.
348 Similar to JEV ISA, we failed to produce Fragment I using three different medium and low copy
349 bacterial plasmids. Subdividing the toxic Fragment I into three sub-fragments (A, B, and c) did
350 not work because the sub-fragment Fragment I-c was also toxic to bacteria (**Table S1**).
351 Subsequently, we divided the highly toxic WNV-Per Fragment I into four sub-fragments, each
352 smaller than 1.8 kb. This allowed the *synthesis of DNA* commercial production process that is
353 bacteria-free (**Table S1**).
354
355 While various approaches have been employed to overcome technical difficulties in constructing
356 cDNA molecules representing the full-length flavivirus genomes in bacterial vectors, this process
357 remains challenging, laborious, and time-consuming. As demonstrated by our difficulties during
358 the rescue of synthetic JEV and WNV (**Table S1**), these challenges are also present in the
359 classical ISA approach. We propose that subdividing toxic fragments into sub-fragments smaller
360 than 1.8 kb suitable for the *synthesis of DNA* process is currently the most rapid and robust

361 strategy to overcome the need for bacterial plasmids and bacteria and ensure the fast rescue of
362 entirely synthetic flaviviruses.
363 This strategy significantly shortens the time required to produce recombinant flaviviruses. For
364 example, the *synthesis of DNA* process by a commercial supplier (**Table S1**) has turnaround time
365 2-4 days. Additionally, the synthesis of DNA is cost-effective with current 0.07 USD per bp; for
366 example, 4.3 kb DNA fragment for WNV ISA ordered via *synthetic clonal genes* process with
367 bacterial plasmids and amplification in bacteria costs around 840 USD with 3-4 weeks
368 turnaround time, while the same fragment divided into four sub-fragments and ordered via
369 bacteria-free *synthesis of DNA* costs 360 USD with 2-4 days turnaround time. During production,
370 the provider flanks DNA fragments with short 22 bp adapters (**File S1**), facilitating efficient PCR
371 amplification of ordered ISA fragments from the provided construct. The provider also applies
372 NGS to verify correct sequences, reducing both time and costs for virus rescue. We anticipate
373 that ongoing improvements in DNA synthesis technology and associated cost reductions will
374 provide even faster and more cost-effective bacteria-free fragments for ISA, enabling the even
375 more rapid production of entirely synthetic flaviviruses.
376
377 The zinc finger CCCH-type antiviral protein 1, also known as ZAP, ZC3HAV1, or PARP13, is a
378 cellular protein with broad antiviral activity. ZAP binds viral RNA and evokes antiviral activity
379 by mediating viral RNA degradation and translational inhibition [47]. It also interacts with
380 various cellular proteins that may act as co-factors, enhancing its antiviral effects [48].
381 Furthermore, ZAP can augment other antiviral systems [44,49]. Recent studies, including our
382 own, have demonstrated that flaviviruses such as Zika virus, JEV, and WNV are susceptible to
383 ZAP antiviral effects in VERO cells [44-46]. Thus, we also compared the efficacy of JEV-WT.

384 JEV-CpG, and WNV-Per ISA in ZAP-WT and ZAP-KO cells. Both cell types showed 100%
385 efficiency, with viruses rescued in all five replicates. However, the increased number of virus-
386 positive cells and infectious titers in ZAP-KO cells suggests that these cells may be more
387 effective for rescuing modified flaviviruses, such as attenuated variants for live attenuated
388 vaccines, including CpG-enriched vaccines. This is significant because CpG dinucleotide
389 enrichment is a novel vaccine approach. Increasing CpG dinucleotides in viral RNA, while
390 preserving the original amino acid composition, may weaken the virus, preventing disease but
391 potentially inducing strong antiviral immunity. However, CpG-enriched vaccine candidates are
392 attenuated both *in vitro* and *in vivo*, which can complicate their rescue and the generation of
393 high-titer vaccine stocks [27,28]. Using VERO-ZAP-KO cells could aid in developing CpG-
394 enriched vaccine candidates, and it is advantageous that VERO cells are already used as a GMP
395 line for producing many vaccines.

396

397 In conclusion, the ISA method is a robust and straightforward approach to reverse genetics for
398 JEV and WNV. In this study, we validated a modified ISA strategy that involves subdividing the
399 toxic DNA fragment into four short overlapping sub-fragments, each up to 1.8 kb, for subsequent
400 bacteria-free *DNA synthesis* production. To our knowledge, this strategy had never been applied
401 to ISA before, enabling the rapid generation of flaviviruses using a completely synthetic method
402 for toxic ISA flavivirus fragments. The strategy can be particularly beneficial for research on
403 emerging flaviviruses where a rapid response is needed to rescue new virus variants during
404 outbreaks.

405

ETHICS APPROVAL STATEMENT

The animal studies were approved by The Ohio State University Institutional Biosafety Committee (e-Protocol # 2022R00000111) and The Institutional Animal Care and Use Committee (e-Protocol #2023A00000095).

DISCLOSURE STATEMENT

The authors declare that the research was conducted in the absence of any commercial or financial relationships that could be construed as a potential conflict of interest.

AUTHOR CONTRIBUTIONS

Conceptualization: PPS, NPKL, UK. Investigation: PPS, NPKL, UK. Data analysis: PPS, NPKL, UK. Funding: UK. Writing—original draft preparation: PPS, NPKL, UK. Writing—review and editing: PPS, NPKL, UK.

DATA AVAILABILITY

All data are available in the manuscript or in the supplemental data.

FUNDING

PPS received a Scholarship from the School of Public Health, University of Saskatchewan. The funder had no role in study design, data collection and analysis, decision to publish, or manuscript preparation.

429 **REFERENCES**

430 1. Pierson TC, Diamond MS. The continued threat of emerging flaviviruses. Nat Microbiol. 2020
431 Jun;5(6):796-812.
432 2. Blackburn NK, Swanepoel R. An investigation of flavivirus infections of cattle in Zimbabwe
433 Rhodesia with particular reference to Wesselsbron virus. J Hyg (Lond). 1980 Aug;85(1):1-33.
434 3. Bhatt S, Gething PW, Brady OJ, et al. The global distribution and burden of dengue. Nature. 2013
435 Apr 25;496(7446):504-7.
436 4. Gubler DJ. Dengue/dengue haemorrhagic fever: history and current status. Novartis Found
437 Symp. 2006;277:3-16; discussion 16-22, 71-3, 251-3.
438 5. Amicizia D, Zangrillo F, Lai PL, et al. Overview of Japanese encephalitis disease and its prevention.
439 Focus on IC51 vaccine (IXIARO®). Journal of Preventive Medicine and Hygiene2018. p. E99-E107.
440 6. Tarantola A, Goutard F, Newton P, et al. Estimating the burden of Japanese encephalitis virus and
441 other encephalitides in countries of the mekong region. In: Gray DJ, editor. PLoS neglected
442 tropical diseases2014. p. e2533.
443 7. Chaturvedi UC, Mathur A, Chandra A, et al. Transplacental Infection with Japanese Encephalitis
444 Virus. Journal of Infectious Diseases: Oxford University Press; 1980. p. 712-715.
445 8. Lindquist L. Recent and historical trends in the epidemiology of Japanese encephalitis and its
446 implication for risk assessment in travellers. Journal of Travel Medicine2018. p. S3-S9.
447 9. Oliveira ARS, Piaggio J, Cohnstaedt LW, et al. Introduction of the Japanese encephalitis virus (JEV)
448 in the United States – A qualitative risk assessment. Transboundary and Emerging Diseases2019.
449 p. 1558-1574.
450 10. Huang YJS, Harbin JN, Hettenbach SM, et al. Susceptibility of a North American Culex
451 quinquefasciatus to Japanese Encephalitis Virus. Vector borne and zoonotic diseases (Larchmont,
452 N.Y.): Vector Borne Zoonotic Dis; 2015. p. 709-711.
453 11. Faizah AN, Kobayashi D, Matsumura R, et al. Blood meal source identification and RNA virome
454 determination in Japanese encephalitis virus vectors collected in Ishikawa Prefecture, Japan,
455 show distinct avian/mammalian host preference. J Med Entomol. 2023 Apr 7.
456 12. Shimizu T, Kawakami Y, Fukuhara S, et al. Experimental stillbirth in pregnant swine infected with
457 Japanese encephalitis virus. The Japanese journal of experimental medicine1954. p. 363-375.
458 13. Howard-Jones AR, Pham D, Jeoffreys N, et al. Emerging Genotype IV Japanese Encephalitis Virus
459 Outbreak in New South Wales, Australia. Viruses. 2022 Aug 24;14(9).
460 14. Barrett ADT. West Nile in Europe: an increasing public health problem. J Travel Med. 2018 Jan
461 1;25(1).
462 15. Petersen LR, Carson PJ, Biggerstaff BJ, et al. Estimated cumulative incidence of West Nile virus
463 infection in US adults, 1999-2010. Epidemiol Infect. 2013 Mar;141(3):591-5.
464 16. Neumann G, Kawaoka Y. Reverse genetics systems for the generation of segmented negative-
465 sense RNA viruses entirely from cloned cDNA. Curr Top Microbiol Immunol. 2004;283:43-60.
466 17. Aubry F, Nougairede A, Gould EA, et al. Flavivirus reverse genetic systems, construction
467 techniques and applications: a historical perspective. Antiviral Res. 2015 Feb;114:67-85.
468 18. Ruggli N, Rice CM. Functional cDNA clones of the Flaviviridae: strategies and applications. Adv
469 Virus Res. 1999;53:183-207.
470 19. Park CJ, Lee YA, Yoo SM, et al. Efficient reverse genetics approach involving infectious
471 subgenomic amplicon for engineering dengue virus. J Med Virol. 2023 Aug;95(8):e28978.
472 20. Gritsun TS, Gould EA. Infectious transcripts of tick-borne encephalitis virus, generated in days by
473 RT-PCR. Virology. 1995 Dec 20;214(2):611-8.
474 21. Rice CM, Grakoui A, Galler R, et al. Transcription of infectious yellow fever RNA from full-length
475 cDNA templates produced by in vitro ligation. New Biol. 1989 Dec;1(3):285-96.

476 22. Kapoor M, Zhang L, Mohan PM, et al. Synthesis and characterization of an infectious dengue
477 virus type-2 RNA genome (New Guinea C strain). Gene. 1995 Sep 11;162(2):175-80.
478 23. Sumiyoshi H, Hoke CH, Trent DW. Infectious Japanese encephalitis virus RNA can be synthesized
479 from in vitro-ligated cDNA templates. J Virol. 1992 Sep;66(9):5425-31.
480 24. Aubry F, Nougairède A, de Fabritus L, et al. Single-stranded positive-sense RNA viruses generated
481 in days using infectious subgenomic amplicons. The Journal of general virology2014. p. 2462-7.
482 25. Cochin M, Driouich JS, Moureau G, et al. In vivo rescue of arboviruses directly from subgenomic
483 DNA fragments. Emerg Microbes Infect. 2024 Dec;13(1):2356140.
484 26. Trus I, Berube N, Jiang P, et al. Zika Virus with Increased CpG Dinucleotide Frequencies Shows
485 Oncolytic Activity in Glioblastoma Stem Cells. Viruses: Multidisciplinary Digital Publishing
486 Institute; 2020. p. 579.
487 27. Trus I, Udenze D, Berube N, et al. CpG-Recoding in Zika Virus Genome Causes Host-Age-
488 Dependent Attenuation of Infection With Protection Against Lethal Heterologous Challenge in
489 Mice. Front Immunol. 2019;10:3077.
490 28. Trus I, Udenze D, Karniychuk U. Generation of CpG-Recoded Zika Virus Vaccine Candidates.
491 Methods in molecular biology (Clifton, N.J.): Methods Mol Biol; 2022. p. 289-302.
492 29. Udenze D, Trus I, Berube N, et al. CpG content in the Zika virus genome affects infection
493 phenotypes in the adult brain and fetal lymph nodes. Front Immunol. 2022;13:943481.
494 30. Hu F, Zhu T, Guo X, et al. Generation of duck Tembusu virus using a simple reverse genetic system
495 in duck embryo fibroblast cells. J Virol Methods. 2022 Feb;300:114385.
496 31. Hoornweg TE, Godeke GJ, Hoogerwerf MN, et al. Rescue and in vitro characterization of a
497 divergent TBEV-Eu strain from the Netherlands. Sci Rep. 2023 Feb 18;13(1):2872.
498 32. Atieh T, Nougairède A, Klitting R, et al. New reverse genetics and transfection methods to rescue
499 arboviruses in mosquito cells. Scientific Reports: Nature Publishing Group; 2017. p. 13983.
500 33. Driouich JS, Moureau G, de Lamballerie X, et al. Reverse Genetics of RNA Viruses: ISA-Based
501 Approach to Control Viral Population Diversity without Modifying Virus Phenotype. Viruses. 2019
502 Jul 20;11(7).
503 34. Atieh T, Baronti C, de Lamballerie X, et al. Simple reverse genetics systems for Asian and African
504 Zika viruses. Scientific reports: Nature Publishing Group; 2016. p. 39384.
505 35. Touret F, Gilles M, Klitting R, et al. Live Zika virus chimeric vaccine candidate based on a yellow
506 fever 17-D attenuated backbone. Emerg Microbes Infect. 2018 Sep 26;7(1):161.
507 36. Klitting R, Roth L, Rey FA, et al. Molecular determinants of Yellow Fever Virus pathogenicity in
508 Syrian Golden Hamsters: one mutation away from virulence. Emerg Microbes Infect. 2018 Mar
509 29;7(1):51.
510 37. Fiacre L, Nougairede A, Migne C, et al. Different viral genes modulate virulence in model
511 mammal hosts and Culex pipiens vector competence in Mediterranean basin lineage 1 West Nile
512 virus strains. Front Microbiol. 2023;14:1324069.
513 38. Aubry F, Nougairède A, de Fabritus L, et al. “ISA-Lation” of Single-Stranded Positive-Sense RNA
514 Viruses from Non-Infectious Clinical/Animal Samples. In: Ng LFP, editor. PLOS ONE: Public Library
515 of Science; 2015. p. e0138703.
516 39. Takata MA, Goncalves-Carneiro D, Zang TM, et al. CG dinucleotide suppression enables antiviral
517 defence targeting non-self RNA. Nature. 2017 Oct 5;550(7674):124-127.
518 40. Liu J, Jing W, Fang Y, et al. The Infection of the Japanese Encephalitis Virus SA14-14-2 Strain
519 Induces Lethal Peripheral Inflammatory Responses in IFNAR Deficiency Mice. Frontiers in
520 microbiology: Front Microbiol; 2022.
521 41. Zhang YN, Li N, Zhang QY, et al. Rational design of West Nile virus vaccine through large
522 replacement of 3' UTR with internal poly(A). EMBO Mol Med. 2021 Sep 7;13(9):e14108.

42. Daffis S, Samuel MA, Keller BC, et al. Cell-specific IRF-3 responses protect against West Nile virus infection by interferon-dependent and -independent mechanisms. PLoS Pathog. 2007 Jul 27;3(7):e106.
43. Daffis S, Samuel MA, Suthar MS, et al. Interferon regulatory factor IRF-7 induces the antiviral alpha interferon response and protects against lethal West Nile virus infection. J Virol. 2008 Sep;82(17):8465-75.
44. Nguyen Phuong Khanh Le PPS, Ahmad Jawad Sabir, Ivan Trus, Uladzimir Karniychuk. Endogenous ZAP is associated with altered global cellular gene expression during Zika virus infection. bioRxiv. 2024.
45. Chiu HP, Chiu H, Yang CF, et al. Inhibition of Japanese encephalitis virus infection by the host zinc-finger antiviral protein. PLoS Pathogens: Public Library of Science; 2018.
46. Sabir AJ, Le NPK, Singh PP, et al. Endogenous ZAP affects Zika virus RNA interactome. RNA Biol. 2024 Jan;21(1):1-10.
47. Li MMH, Aguilar EG, Michailidis E, et al. Characterization of Novel Splice Variants of Zinc Finger Antiviral Protein (ZAP). J Virol. 2019 Sep 15;93(18).
48. Goodier JL, Pereira GC, Cheung LE, et al. The Broad-Spectrum Antiviral Protein ZAP Restricts Human Retrotransposition. PLOS Genetics: Public Library of Science; 2015. p. e1005252.
49. Nguyen LP, Aldana KS, Yang E, et al. Alphavirus Evasion of Zinc Finger Antiviral Protein (ZAP) Correlates with CpG Suppression in a Specific Viral nsP2 Gene Sequence. Viruses. 2023 Mar 24;15(4).

560 **FIGURE LEGENDS**

561 **Figure 1. Classical ISA method for dengue virus.**
562
563
564 **Figure 2. Dengue virus ISA and stock generation**. (**A**) Cytopathic effect in DENV ISA-
565 transfected ZAP-KO BHK+VERO cells, passage 0 day 7 after transfection. All five replicate wells
566 showed CPE at passages 0 and 1; the representative images are shown. (**B**) Infectious $TCID_{50}$ titers
567 of the DENV stock produced in ZAP-KO cells. The stock was titrated in VERO-ZAP-WT or
568 VERO-ZAP-KO cells. (**C**) DENV RNA loads of the stock determined by virus-specific RT-qPCR.
569 (**D**) Images of cells positive for the DENV E protein (red staining) at 7 days after infection with
570 MOI 0.01. Magnification x200. The experiment was done in 4 replicates. Figures represent the
571 general patterns in all replicates.
572
573
574 **Figure 3. The adapted ISA method for Japanese encephalitis virus.** To overcome toxicity, we
575 divided the toxic Fragment I into two sub-fragments (**Table S1**, **File S1**).
576
577
578 **Figure 4. JEV ISA and stock generation**. Cytopathic effect in JEV-WT (**A**) and JEV-CpG (**D**)
579 ISA-transfected ZAP-KO BHK+VERO cells, passage 0, day 6 after transfection. All five replicates
580 showed CPE; the representative images are shown. Infectious $TCID_{50}$ titers of the JEV-WT (**B**)
581 and JEV-CpG (**E**) stocks produced in ZAP-KO cells. The stock was titrated in VERO-ZAP-WT
582 or VERO-ZAP-KO cells. JEV RNA loads of the stock determined by virus-specific RT-qPCR.
583 Images of cells positive for the JEV-WT (**C**) and JEV-CpG (**G**) E protein (red staining) at 3 days
584 after infection, MOI 0.01. Magnification x200. The experiment was done in 3 biological replicates.
585 Figures represent the general staining patterns in replicates. (**F**) The fold increase of JEV-WT or
586 JEV-CpG RNA loads in cell supernatants collected at 1h and 72h after inoculation. VERO-WT
587 and VERO-ZAP-KO cells were inoculated with MOI 0.01. Virus inoculums were removed and
588 replaced with media. Supernatants were collected at 1h (to normalize for leftover inoculum RNA)
589 and at 72h. Three biological x 3 technical replicates. ***P=0.0017; unpaired t-test. (**H**) Mean body
590 weight and survival in MOCK *Ifnar1*$^{-/-}$ mice and *Ifnar1*$^{-/-}$ mice injected with the ISA-derived JEV-
591 WT or JWV-CpG. The following clinical scoring was used: 0—no visible abnormalities; 1—mild
592 ataxia or tremors; 2—obvious ataxia or tremors; 3—depression, hunching, reluctance to walk, and
593 falling to the side when walking; 4—close to moribund but still somewhat responsive; 5—
594 paralysis; 6—loos of 20% baseline body weight; 7—found dead. Scores 4, 5, or 6 were used for
595 the endpoint and mouse euthanasia. In body weight a standard error of the mean (SEM) is shown.
596 (**I**) JEV loads in mouse spleen and brain sampled at euthanasia due to severe clinical signs or at
597 the end of the study—at 12 days after injection.
598
599
600 **Figure 5. The adapted ISA method for the wild-type WNV variant (WNV-WT).** To
601 overcome toxicity, we generated Fragment I in the low copy pCC1 bacterial plasmid (**Table S1**,
602 **File S1**).
603
604

605 **Figure 6. The adapted ISA method for the permuted WNV variant (WNV-Per).** To
606 overcome toxicity, we subdivide the toxic Fragment I into four sub-fragments for bacteria-free
607 *synthesis of DNA* production (**Table S1**, **File S1**).
608
609 **Figure 7. WNV ISA and stock generation**. Cytopathic effect in WNV-WT (**A**) and WNV-Per
610 (**B**) ISA-transfected ZAP-KO BHK+VERO cells, passage 0, day 6 after transfection. All five
611 replicates for each WNV variant showed CPE; representative images are shown. Infectious $TCID_{50}$
612 titers and RT-qPCR RNA loads of the WNV-WT (**C**) and WNV-Per (**D**) stocks produced in ZAP-
613 KO cells. For $TCID_{50}$ virus stocks were titrated in VERO-ZAP-WT or VERO-ZAP-KO cells.
614 Images of cells positive for the WNV-WT (**E**) and WNV-Per (**F**) E protein (red staining) at 3 days
615 after infection, MOI 0.01. Magnification x200. The experiment was done in 3 biological replicates.
616 Figures represent the general patterns in all replicates. (**G**) Mean body weight and survival in
617 MOCK C57BL/6J mice and C57BL/6J mice injected with the ISA-derived WNV-WT and WNV-
618 Per. The following clinical scoring was used: 0—no visible abnormalities; 1—mild ataxia or
619 tremors; 2—obvious ataxia or tremors; 3—depression, hunching, reluctance to walk, and falling
620 to the side when walking; 4—close to moribund but still somewhat responsive; 5—paralysis; 6—
621 loos of 20% baseline body weight; 7—found dead. Scores 4, 5, or 6 were used for the endpoint
622 and mouse euthanasia. In body weight a standard error of the mean (SEM) is shown. (**H**) WNV
623 loads in mouse spleen and brain sampled at euthanasia due to severe clinical signs or at the end of
624 the study.
625
626 **Figure 8. Comparative ISA in ZAP-WT and ZAP-KO cells**. (**A**) Cytopathic effect in JEV-WT,
627 JEV-CpG, and WNV-Per ISA-transfected ZAP-WT and ZAP-KO BHK+VERO cells, passage 0,
628 day 5 (JEV-WT and JEV-CpG) and day 4 (WNV-Per) after transfection. All five replicates for
629 JEV-WT, JEV-CpG, and WNV-Per showed CPE; the representative images are shown. The digital
630 quantification of JEV-WT (**B**), JEV-CpG (**D**), and WNV-Per (**F**) E protein-positive cells in all 5-
631 well replicates at day 4 (JEV) and day 2 (WNV) during passage 1 of comparative ISA. For
632 technical replicates, three random images were obtained from each well. Examples of JEV-WT,
633 JEV-CpG, and WNV-Per E protein IHC are in **Figures 4C, G,** and **7F**. ***P<0.0001, unpaired t-
634 test. JEV-WT (**C**), JEV-CpG (**E**), and WNV-Per (**J**) infectious $TCID_{50}$ titers in supernatants
635 collected at day 4 (JEV) and day 2 (WNV-Per) during passage 1 of comparative ISA. Data from
636 4-well replicates are shown. **P<0.014-0.017, unpaired t-test.
637
638
639
640 **SUPPORTING INFORMATION CAPTIONS**
641
642 **Supplemental materials and methods**.
643
644 **Table S1** ISA fragments and primers.
645
646 **Table S2** JEV and WNV genomic parameters.
647
648 **File S1** ISA fragments.
649
650 **File S2** JEV-CpG and WNV-Permuted reference sequences.

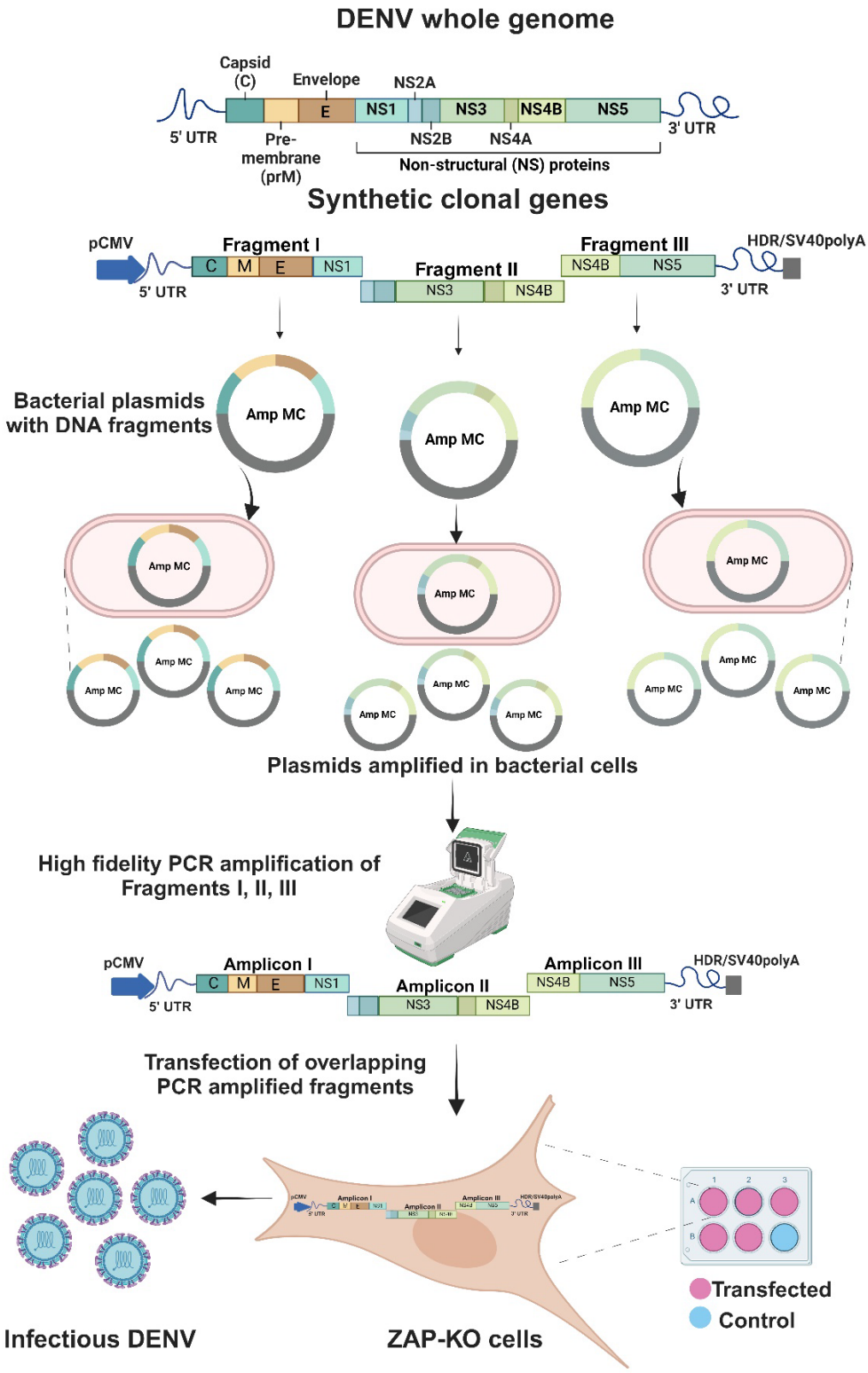
DENV whole genome
Capsid (C)
Envelope
NS2A
E
NS1
NS3
NS4B
NS5
5' UTR
3' UTR
Pre-membrane (prM)
NS2B
NS4A
Non-structural (NS) proteins
Synthetic clonal genes
pCMV
Fragment I
C
M
E
NS1
5' UTR
Fragment II
NS3
NS4B
Fragment III
NS4B
NS5
HDR/SV40polyA
3' UTR
Bacterial plasmids with DNA fragments
Amp MC
Plasmids amplified in bacterial cells
High fidelity PCR amplification of Fragments I, II, III
Amplicon I
Amplicon II
Amplicon III
Transfection of overlapping PCR amplified fragments
Transfected
Control
Infectious DENV
ZAP-KO cells

Fig. 1

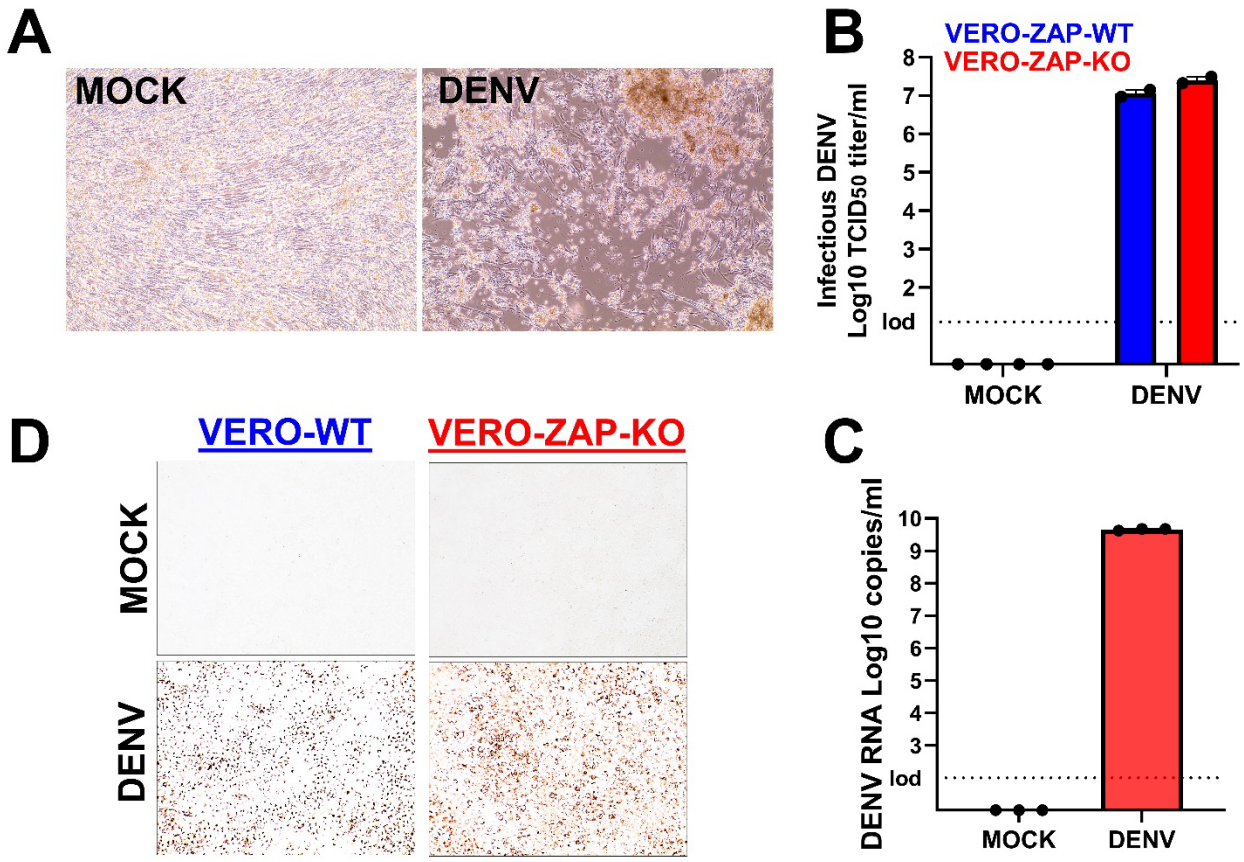
A
MOCK
DENV
B
VERO-ZAP-WT
VERO-ZAP-KO
Infectious DENV
Log10 TCID50 titer/ml
8
7
6
5
4
3
2
lod
MOCK
DENV
D
VERO-WT
VERO-ZAP-KO
MOCK
DENV
C
DENV RNA Log10 copies/ml
10
9
8
7
6
5
4
3
lod
MOCK
DENV

Fig. 2

678

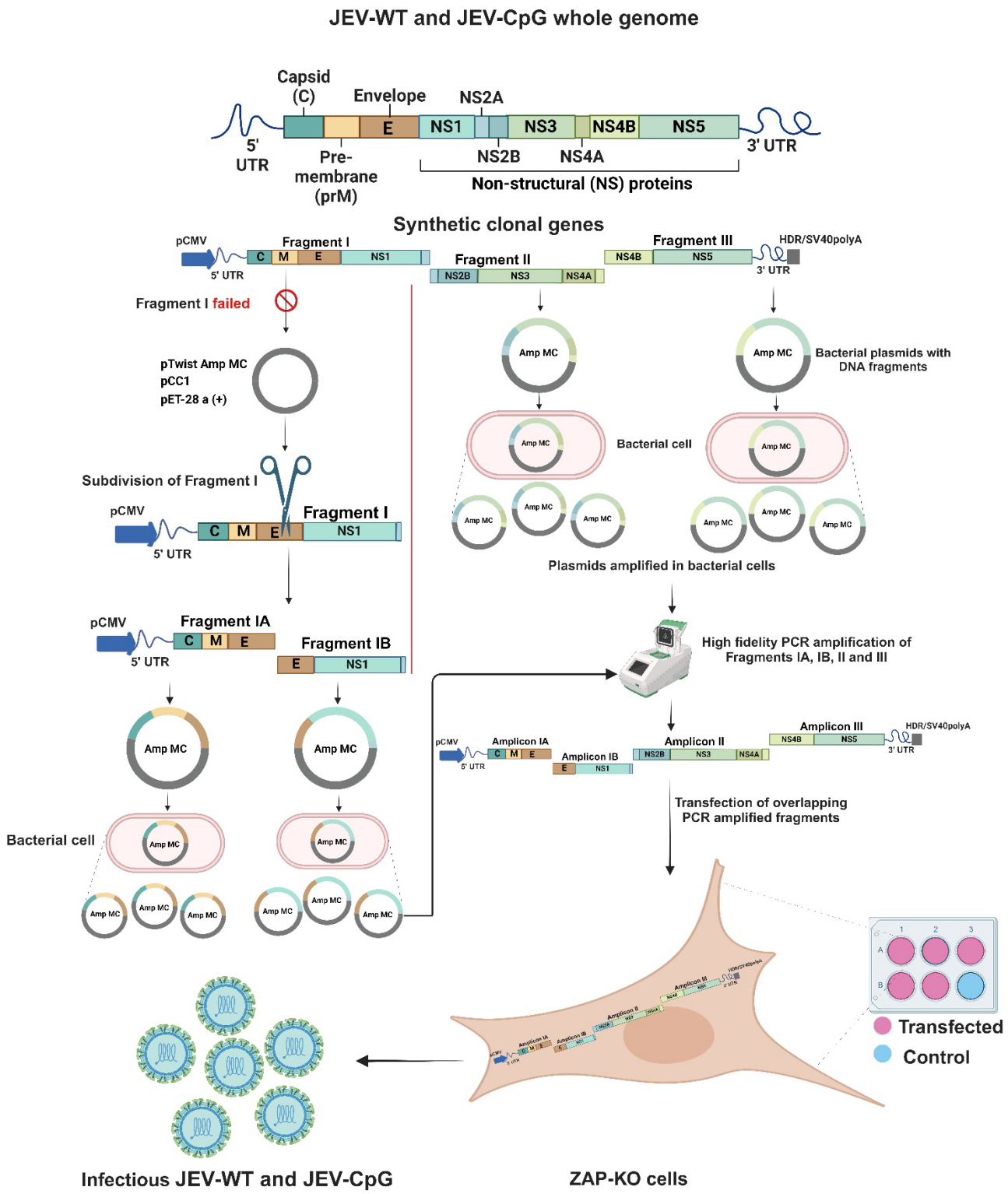

679
680
681

Fig. 3

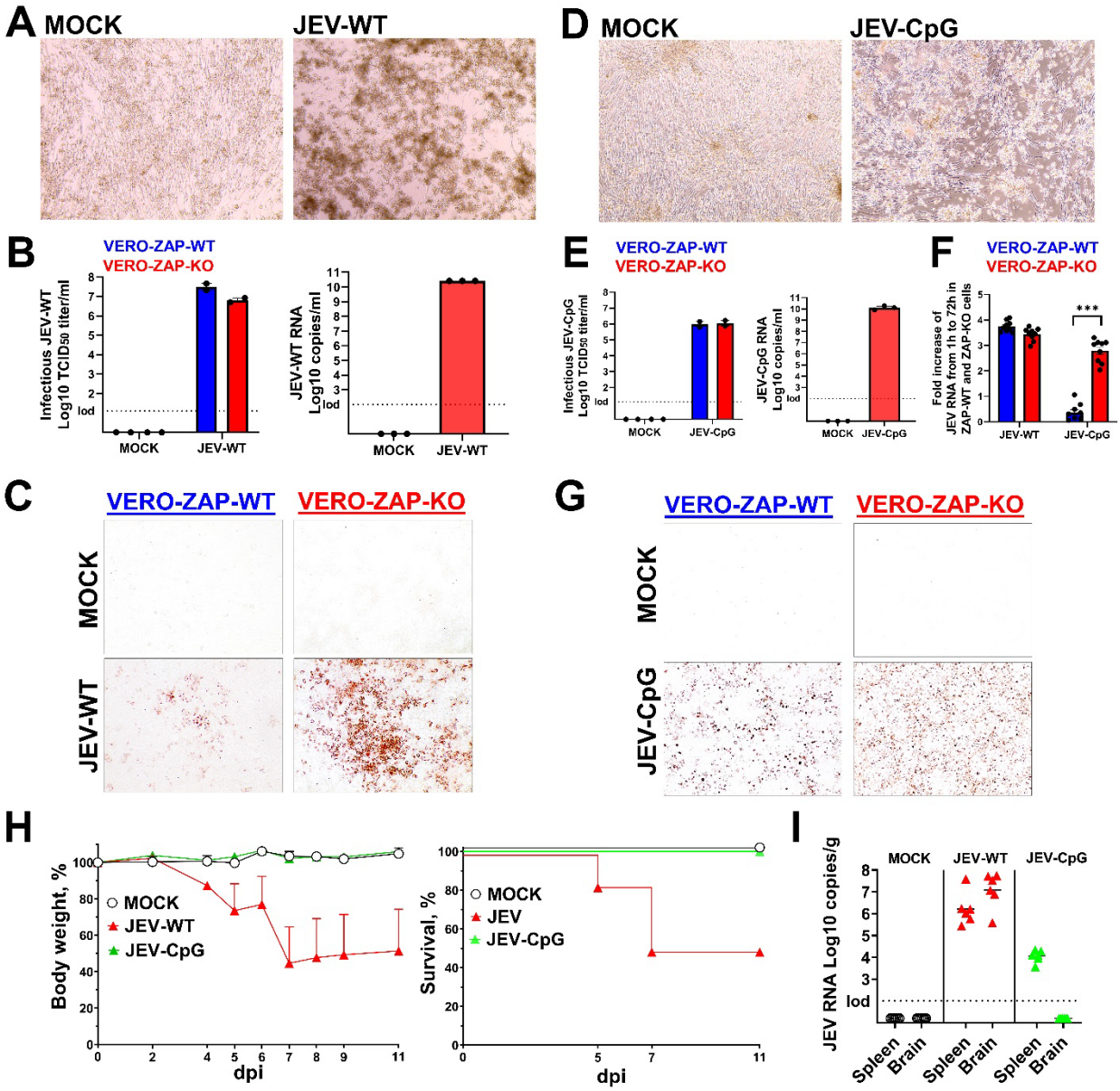
A
MOCK
JEV-WT
D
MOCK
JEV-CpG
B
VERO-ZAP-WT
VERO-ZAP-KO
Infectious JEV-WT Log10 TCID50 titer/ml
lod
MOCK
JEV-WT
JEV-WT RNA Log10 copies/ml
E
Infectious JEV-CpG Log10 TCID50 titer/ml
JEV-CpG
JEV-CpG RNA Log10 copies/ml
F
Fold increase of JEV RNA from 1h to 72h in ZAP-WT and ZAP-KO cells
***
C
G
H
Body weight, %
dpi
Survival, %
JEV
I
JEV RNA Log10 copies/g
Spleen
Brain

Fig. 4

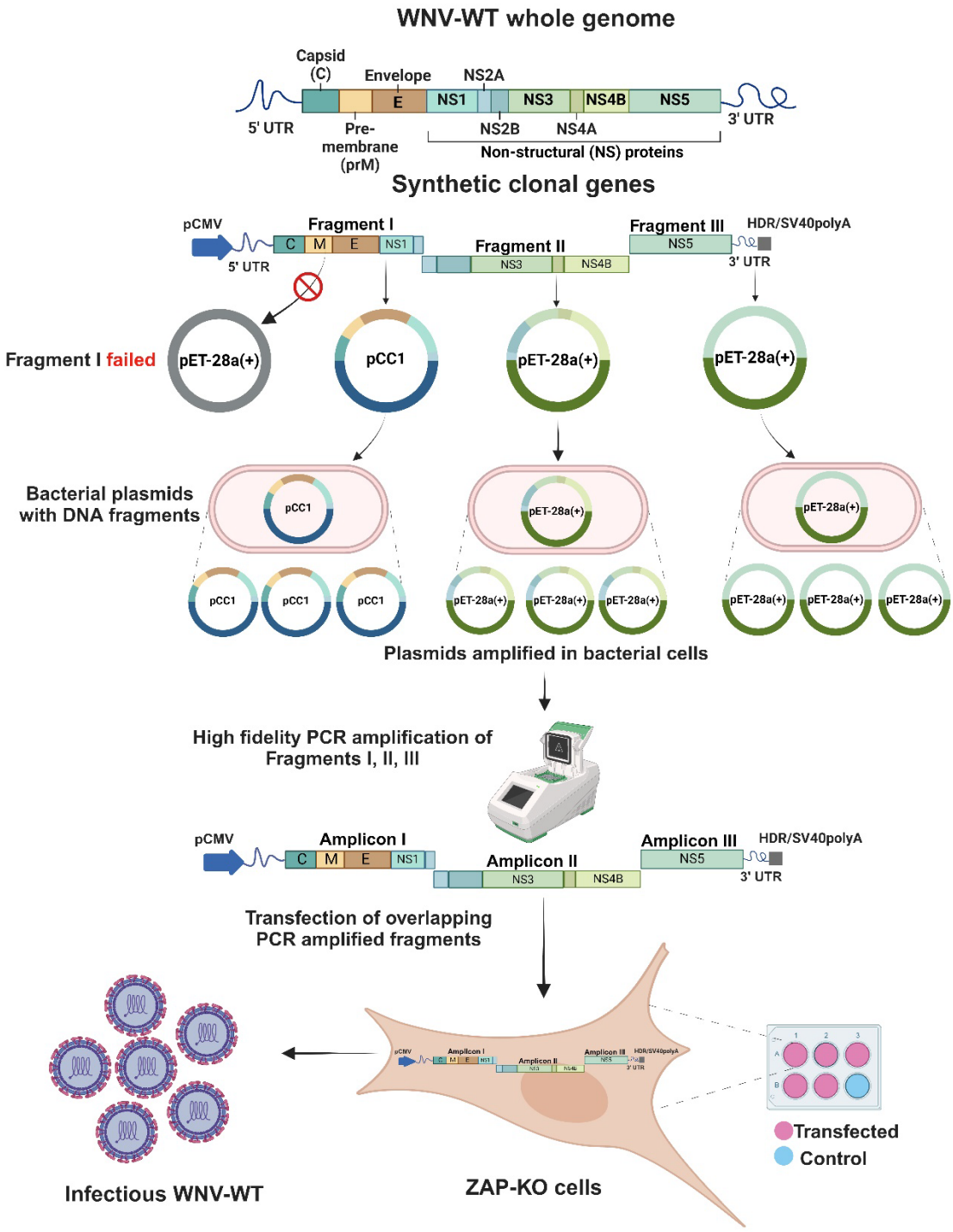
WNV-WT whole genome
Capsid (C)
Envelope
NS2A
E
NS1
NS3
NS4B
NS5
5' UTR
Pre-membrane (prM)
NS2B
NS4A
3' UTR
Non-structural (NS) proteins
Synthetic clonal genes
pCMV
Fragment I
C
M
E
NS1
5' UTR
Fragment II
NS3
NS4B
Fragment III
NS5
HDR/SV40polyA
3' UTR
Fragment I failed
pET-28a(+)
pCC1
pET-28a(+)
pET-28a(+)
Bacterial plasmids with DNA fragments
pCC1
pET-28a(+)
pET-28a(+)
pCC1
pCC1
pCC1
pET-28a(+)
pET-28a(+)
pET-28a(+)
pET-28a(+)
pET-28a(+)
pET-28a(+)
Plasmids amplified in bacterial cells
High fidelity PCR amplification of Fragments I, II, III
pCMV
Amplicon I
C
M
E
NS1
Amplicon II
NS3
NS4B
Amplicon III
NS5
HDR/SV40polyA
3' UTR
Transfection of overlapping PCR amplified fragments
Infectious WNV-WT
ZAP-KO cells
Transfected
Control

Fig. 5

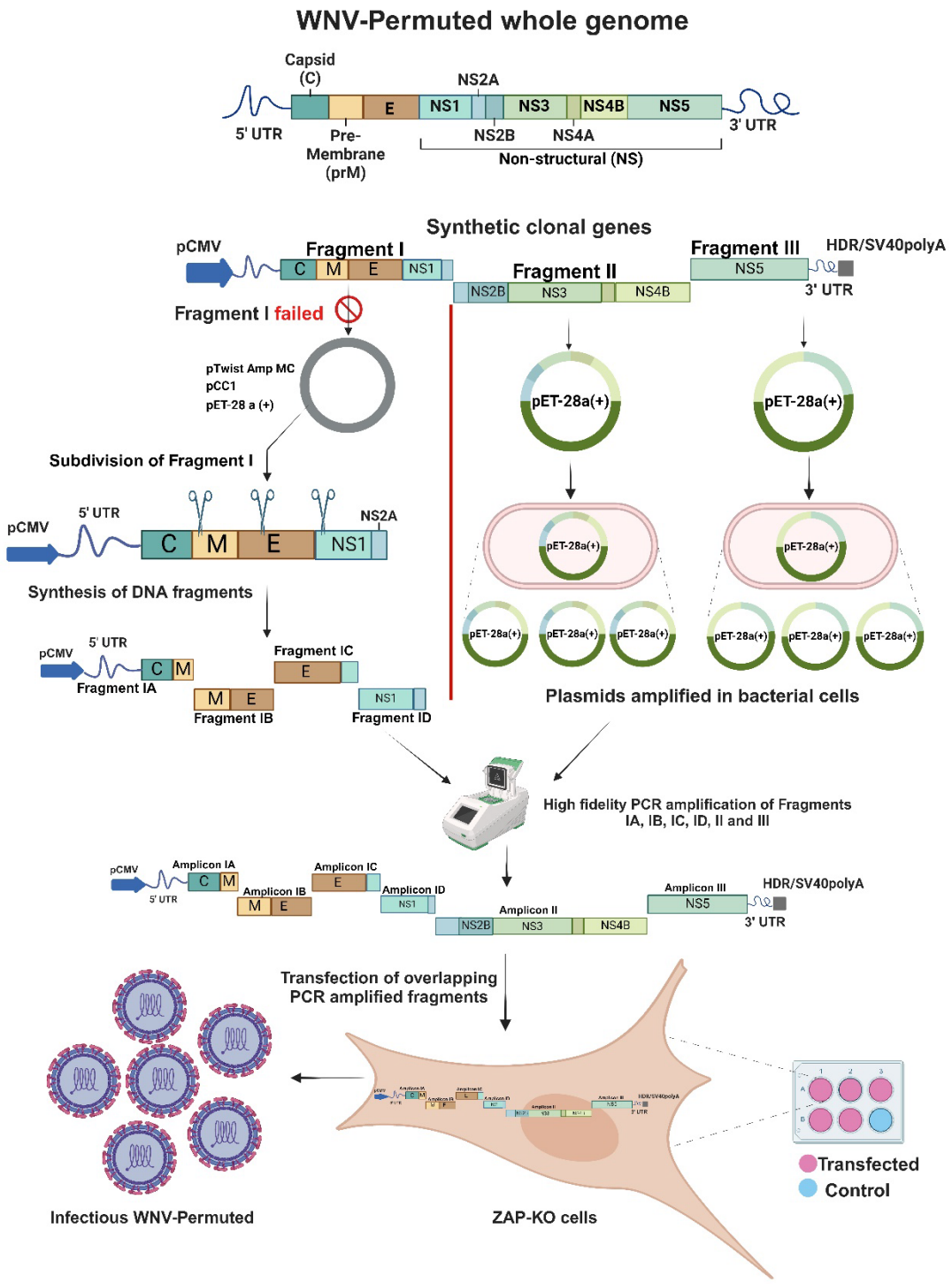
WNV-Permuted whole genome
Capsid (C)
NS2A
5' UTR
Pre-Membrane (prM)
E
NS1
NS3
NS4B
NS5
3' UTR
NS2B
NS4A
Non-structural (NS)
Synthetic clonal genes
pCMV
Fragment I
C
M
E
NS1
Fragment II
NS2B
NS3
NS4B
Fragment III
NS5
HDR/SV40polyA
3' UTR
Fragment I failed
pTwist Amp MC
pCC1
pET-28 a (+)
pET-28a(+)
Subdivision of Fragment I
5' UTR
NS2A
Synthesis of DNA fragments
Fragment IA
Fragment IB
Fragment IC
Fragment ID
Plasmids amplified in bacterial cells
High fidelity PCR amplification of Fragments IA, IB, IC, ID, II and III
Amplicon IA
Amplicon IB
Amplicon IC
Amplicon ID
Amplicon II
Amplicon III
Transfection of overlapping PCR amplified fragments
Transfected
Control
Infectious WNV-Permuted
ZAP-KO cells

Fig. 6

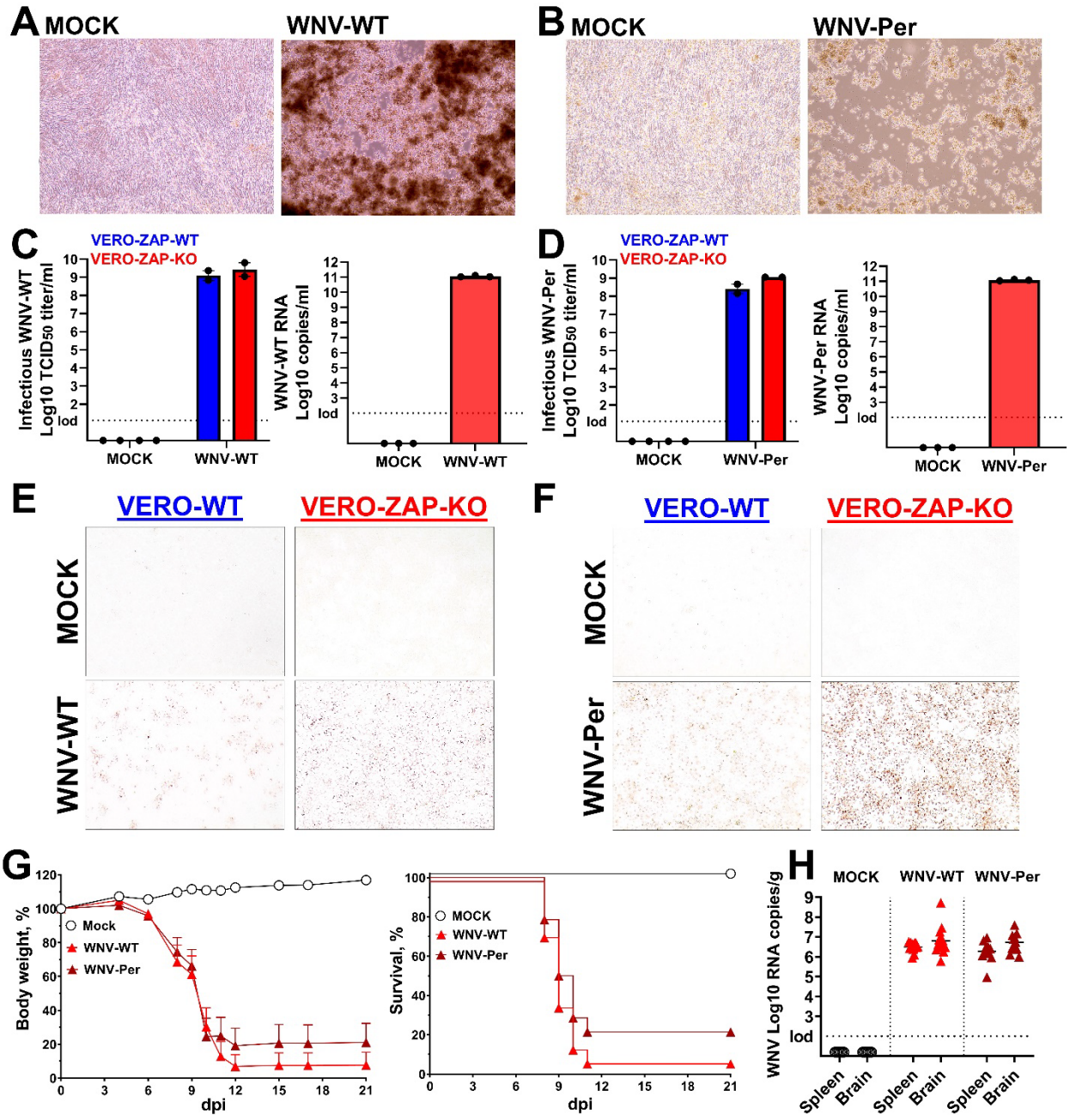
A MOCK
WNV-WT
B MOCK
WNV-Per
C
VERO-ZAP-WT
VERO-ZAP-KO
Infectious WNV-WT Log10 TCID50 titer/ml
lod
MOCK
WNV-WT
WNV-WT RNA Log10 copies/ml
D
Infectious WNV-Per Log10 TCID50 titer/ml
WNV-Per
WNV-Per RNA Log10 copies/ml
E
VERO-WT
VERO-ZAP-KO
MOCK
WNV-WT
F
WNV-Per
G
Body weight, %
Mock
dpi
Survival, %
MOCK
H
WNV Log10 RNA copies/g
Spleen
Brain

Fig. 7

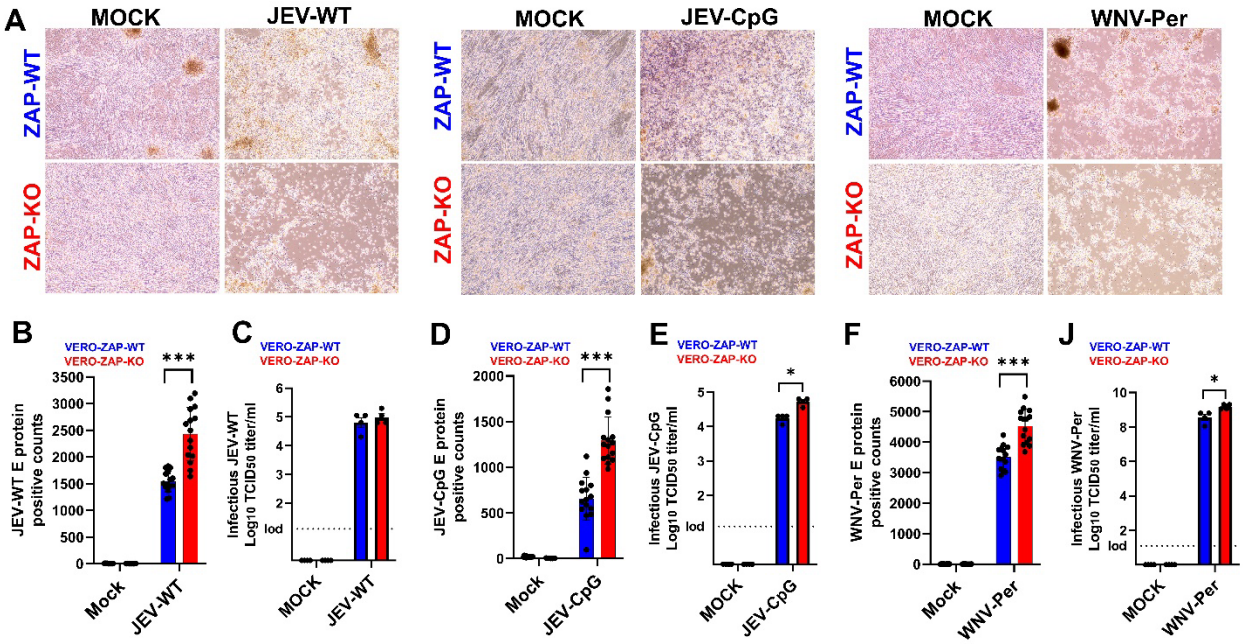
A
MOCK
JEV-WT
MOCK
JEV-CpG
MOCK
WNV-Per
ZAP-WT
ZAP-KO
B
VERO-ZAP-WT
VERO-ZAP-KO
JEV-WT E protein positive counts
Mock
JEV-WT
C
Infectious JEV-WT Log10 TCID50 titer/ml
lod
MOCK
JEV-WT
D
JEV-CpG E protein positive counts
JEV-CpG
E
Infectious JEV-CpG Log10 TCID50 titer/ml
JEV-CpG
F
WNV-Per E protein positive counts
WNV-Per
J
Infectious WNV-Per Log10 TCID50 titer/ml
WNV-Per

Fig. 8

SUPPLEMENTAL MATERIALS AND METHODS

Infectious subgenomic amplicon strategies for Japanese encephalitis and West Nile viruses

Prince Pal Singh[1,2], Nguyen Phuong Khanh Le[1], Uladzimir Karniychuk[1,*]

[1]Department of Veterinary Biosciences, College of Veterinary Medicine, The Ohio State University, Columbus, OH, USA

[2]School of Public Health, University of Saskatchewan, Saskatoon, Canada

***Correspondence:** Uladzimir Karniychuk

Department of Veterinary Biosciences, College of Veterinary Medicine, The Ohio State University, Columbus, OH, USA

karniychuk.1@osu.edu

SUPPLEMENTAL MATERIALS AND METHODS

Cells

We maintained wild-type VERO E6 (VERO-ZAP-WT) and BHK-21 (BHK-ZAP-WT) cells, along with CCCH-type zinc finger antiviral protein (ZAP) knockout (ZAP-KO) derivatives (VERO-ZAP-KO and BHK-ZAP-KO), in DMEM (Fisher, MA, USA; #11-965-118) supplemented with 10% heat-inactivated fetal bovine serum (FBS, Fisher, MA, USA; #A5256801), 1x Penicillin-Streptomycin (Fisher, MA, USA; #15140122), and 2.67 mM sodium bicarbonate (Fisher, MA, USA; # 25080094) at +37°C in a 5% CO_2 humidified incubator.

To generate the VERO-ZAP-KO cell line, we previously used the guide RNA (gRNA) GTCTCTGGCAGTACTTGCGA targeting the first exon of the *Chlorocebus sabaeus* (Gene ID: 103226990) ZC3HAV1 gene, necessary for expressing all ZAP isoforms. A non-targeting gRNA (ACGGAGGCTAAGCGTCGCAA) served as the control [1,2]. These gRNAs were transiently transfected into cells using GenCrispr NLS-Cas9-NLS Nuclease (GenScript). Transfected cells were then seeded in 96-well plates through limiting dilution to generate isogenic single clones. After expansion, the clones were genotyped via Sanger sequencing using primers ATCGCTGGGCTGGACTAACG and GCAGAGAAGGGAGTGGCTGAA to identify location of indels on *Chlorocebus sabaeus* genome: -2 bp deletion, NW_023666072.1: 4677550-4677551. The knockout subclone confirmed by genotyping was further validated by western blot for ZAP expression in our previous studies [1,2]. Negative control cells were not isolated into single clones but were validated by Sanger sequencing to confirm the absence of indels.
The same strategy was used to generate BHK-ZAP-KO cells with gRNA GGAGATCGTAGGCCAGACCGGGG targeting the first exon of the *Mesocricetus auratus*

47 (Gene ID: 110343172) Zc3hav1 gene and the same non-targeting control gRNA. After
48 expansion, the clones were genotyped via Sanger sequencing with primers
49 GCTGCTTCATCACCAAGATCC and GGTCGGGAAGACCCTTTCAC to identify location of
50 indels on *Mesocricetus auratus* genome: -29 bp deletion, NW_024429200.1: 3564916-3564944.
51 We confirmed the absence of mycoplasma contamination in all cells using the LookOut
52 Mycoplasma PCR Detection Kit (Millipore Sigma, MA, USA; #MP0035).
53

54 ***In silico* CpG enrichment and permutation in viral genomes**

55 For CpG dinucleotide enrichment in the JEV genome, specifically in the region encoding the E
56 protein (**File S2**), we used the SSE 1.3 software package [3], as we previously described [4,5].
57 The genomic parameters of the wild-type and CpG-enriched JEV variants are listed in **Table S2**.
58

59 Certain experiments involving viral genomic mutations need permuted or scrambled virus
60 control variants. Permutation can potentially impact the efficiency of reverse genetics methods.
61 To simulate this scenario for ISA, we generated a permuted control for WNV. For permutation
62 of WNV sequences we selected genomic regions encoding E and NS1 (**File S2**) because these
63 proteins are important for flavivirus pathogenesis, modulation of the infection cycle, viral RNA
64 replication, and host immune evasion. Moreover, we previously permuted these genomic regions
65 in the Zika virus genome; this permutation did not affect Zika infection phenotypes *in vitro* and
66 in mice [4]. We used an SSE 1.3 software package [3], specifically the CDLR randomizing in the
67 SSE 1.3 [3,6-8]. During randomization we sought to avoid areas of the genome containing RNA
68 elements that are required for replication or translation of the virus genome, such as cis-
69 replicating elements, gene start or gene-end signals; we also avoided regions with prominent

70 secondary structures. The CDLR randomizes the order of codons within the sequence while
71 maintaining encoded proteins, dinucleotide frequencies, and coding parameters (**Table S2**).
72
73 **Infectious-Subgenomic-Amplicons (ISA) and virus stock generation**
74 The following reference sequences were used for *de novo* synthesis of flaviviruses: DENV type 2
75 strain 16681 [GenBank: U87411.1], JEV strain SA14-14-2 [GenBank: MK585066.1], and WNV
76 strain NY99 [GenBank: DQ211652.1]. To rescue DENV, JEV, and WNV, initially, we used
77 three overlapping (70-80 nt overlap) ISA DNA fragments (3,371-4,550 bp length) covering the
78 entire viral genome (**Table S1**; **File S1**); three overlapping DNA fragments is common ISA
79 strategy for flaviviruses [9,10]; thus, we consider it as a classical approach. The first and last
80 fragments for each virus are flanked with pCMV promoter and HDR/SV40pA sequences (**File**
81 **S1**).
82
83 Initially all DNA fragments for ISA were ordered through GeneScript (NJ, USA) or Twist
84 Biosciences (CA, USA) *synthetic clonal genes* services where DNA fragments are synthesized,
85 inserted into the bacterial plasmids (**Table S1**), amplified in bacteria, extracted, sequenced, and
86 plasmids with inserted fragments are delivered as lyophilized DNA with known concentration.
87 Some flavivirus ISA DNA fragments were toxic to bacteria, in both medium copy and low copy
88 plasmids (**Table S1**), and after multiple attempts *synthetic clonal genes* approach failed (see
89 results for details). To overcome this flavivirus DNA sequence toxicity to bacteria, we split toxic
90 clonal genes into smaller overlapping fragments below 1.8 kb length. These smaller size
91 fragments allowed *synthesis of DNA* services from Twist Biosciences were DNA fragments,
92 flanked with 22 bp adapters (**File S1**), are rapidly (2-4 days service) synthesized without using

93 bacterial plasmids and bacteria. Twist Biosciences and GeneScript confirmed the correct
94 sequences of DNA fragments by next-generation-sequencing (NGS).
95
96 Overlapping clonal genes or synthetic DNA ISA fragments were amplified with high fidelity
97 Invitrogen Platinum PCR SuperMix High Fidelity (Fisher, MA, USA; #12-532-016) (primers are
98 in **Table S1**), mixed in equimolar concentration to obtain the final 1µg of DNA for transfection,
99 and transfected into BHK-ZAP-KO cell monolayers (6-well plates, five transfection replicates,
100 one mock-transfection control well) with Lipofectamine 3000 (Fisher, MA, USA; #L3000015) in
101 640 µl of OptiMEM (Fisher, MA, USA; #11-058-021) for 12 h at +37°C, 5% CO_2. Afterward,
102 OptiMEM media was removed and replaced with 3 ml of DMEM with 10% of FBS containing
103 $4x10^5$ VERO-ZAP-KO cells on the top of BHK-ZAP-KO cells and incubated plates for
104 additional 6-7 days (passage 0). For passage 1, 400 µl of media from each well of passage 0 was
105 transferred to wells with VERO-ZAP-KO cells and incubated for 4-7 days. During passages 0
106 and 1, cells were monitored for cytopathic effect (CPE). Generated flaviviruses were additionally
107 passaged 2-3 times on VERO-ZAP-KO cells to generate virus stocks; flasks were monitored for
108 CPE. Cell culture media from the final stocks were centrifuged (12,000 g, 20 min, +4°C),
109 aliquoted, and frozen (-80°C). Viral titers were quantified in duplicate in VERO-ZAP-WT and
110 VERO-ZAP-KO cells with endpoint dilution assay described below. The absence of mycoplasma
111 contamination in all virus stocks and cell cultures was confirmed using PCR Detection Kit
112 (Millipore Sigma, MA, USA; #MP0035).
113
114 To validate virus stock sequences, RNA was extracted from virus stock culture supernatants as
115 described below. PCR was performed using SuperScript™ IV One-Step RT-PCR System (Fisher,

116 MA, USA; #12-594-025) as per manufacturer's instructions with the primers targeting sequences
117 encoding E protein: DENV (Forward 5- GACAGCTGTCACTCCTTCAAT GAC-3 and Reverse
118 5- CATGCTCTTCCCCTGAGTGAG G-3); JEV-WT (Forward 5-
119 GTTTTAATTGTCTGGGAATGGGC-3 and Reverse 5-GCCAACTTTGTATTTGATGTTTTC-
120 3); JEV-CpG (Forward 5-CAGTTTTAATTGTCTGGGAATGGG-3 and Reverse 5-
121 GTCAGCATGCACATTGGTCG-3); WNV-WT (Forward 5-
122 CTATTGCTTTTGGTGGCCCCAG-3 and Reverse 5-GTAGTTGGTCCATGGACAAA-3);
123 WNV-Per (Forward 5-CTATTGCTTTTGGTGGCCCCAG-3 and Reverse 5-
124 GTAGTTGGTCCATGGACAAA-3). PCR products were run on a 1% agarose gel, and DNA was
125 purified and concentrated using DNA Clean & Concentrator-5 (Zymo Research, CA, USA; #
126 D4013) as per manufacturer's instructions. DNA was sequenced by Sanger sequencing and
127 sequences were aligned with corresponding ISA sequences (**File S1**). Sanger sequencing
128 confirmed correct sequences in DENV, JEV, and WNV stocks.

129

130 **Comparative ISA**

131 To compare ISA efficiency on ZAP-WT and ZAP-KO cells, JEV and WNV fragments were
132 transfected into ZAP-WT or ZAP-KO cells as above. These experiments were conducted
133 simultaneously; also, the DNA amplicons for transfection in ZAP-WT or ZAP-KO cells were
134 obtained from the same PCR reactions. During passage 0, ZAP-WT and ZAP-KO cells were
135 observed for 5 (JEV variants) and 4 (WNV variants) days to compare CPE; the time was shorter
136 for WNV because it causes more aggressive infection and CPE. During the 1st passage, CPE was
137 observed, supernatants were collected on days 2-4 (2 for WNV variants; 4 for JEV variants) from
138 each well, and infectious virus titers were quantified with the end-point dilution assay as

139 described below. The shorter passage duration in the comparative ISA than in the initial ISA
140 used for virus rescue were applied to preserve cell monolayers for quantitative
141 immunohistochemistry (IHC) described below. The quantitative difference between ZAP-WT
142 and ZAP-KO conditions was represented by $TCID_{50}$ infectious titers in cell culture supernatants
143 from four replicates. Additionally, cellular monolayers from each transfected and mock-
144 transfected well (five replicates) were fixed and stained for viral E protein via IHC as described
145 in the infectious virus titration below. To quantify and compare IHC staining between ZAP-WT
146 and ZAP-KO conditions, three images (magnification x200) were randomly acquired in all five
147 well replicates with the same microscopic settings. Afterward, each image was processed in
148 ImageJ (NIH) (https://imagej.net/imaging/particle-analysis) with Automatic Particle counting
149 [2].
150
151 **Mouse experiments**
152 The animal studies were approved by The Ohio State University Institutional Biosafety
153 Committee (e-Protocol # 2022R00000111) and IACUC (e-Protocol #2023A00000095). Mice
154 were euthanized by deeply anesthetizing them with isoflurane, followed by cervical dislocation.
155
156 We conducted mouse experiments to identify whether ISA-rescued synthetic JEV and WNV
157 cause expected infection phenotypes which were previously described in mice infected with wild
158 or field isolates. The wild SA14-14-2 JEV strain does not cause clinical signs in conventional
159 mice; thus, we used *Ifnar1*$^{-/-}$ mice (The Jackson Laboratory, USA; Strain #:028288). The SA14-
160 14-2 JEV strain causes clinical signs or lethality in infected *Ifnar1*$^{-/-}$ mice [11]. After one week of
161 acclimatization, five-week-old mice (6 mice per group) were injected subcutaneously with the

162 virus-free media (MOCK) or ISA-derived JEV-WT or JEV-CpG variants (**Table S1**). We
163 standardized mouse injection doses by normalization of viral RNA loads (determined by RT-
164 qPCR, see below) in the JEV-WT and JEV-CpG inoculums which resulted in 10^{10} RNA
165 copies/mouse for both variants (JEV-WT – 10^{7} $TCID_{50}$/mouse; JEV-CpG – $10^{6.3}$ $TCID_{50}$/mouse;
166 titers quantified on VERO-ZAP-WT cells, see below). Afterward, mice were monitored for
167 clinical signs and body weight. Mice were sacrificed when exhibiting greater than 20% weight
168 loss or severe clinical signs. We sampled spleen and brain from deceased mice, or from survived
169 mice at the end of the study to quantify JEV loads.
170
171 The wild NY99 WNV strain causes severe infection in conventional C57BL/6J mice; thus, we
172 used the well-characterized C57BL/6J mouse lethal model [12-14]. Five-week-old C57BL/6J
173 mice (Strain #:000664; 14 mice per group) were ordered from The Jackson Laboratory,
174 acclimatized for a week, and injected intraperitoneally (IP) with the virus-free media (MOCK),
175 ISA-derived WNV wild-type (WNV-WT), or ISA-derived WNV permuted (WNV-Per) variant
176 (**Table S1**). We standardized mouse injection doses by normalization of viral RNA loads
177 (determined by RT-qPCR, see below) in the WNV-WT and WNV-Per inoculums which resulted
178 in 10^{7} RNA copies/mouse for both variants (WNV-WT - 10^{5} $TCID_{50}$/mouse; WNV-Permuted -
179 $10^{5.6}$ $TCID_{50}$/mouse; titers quantified on VERO-ZAP-WT cells, see below). Afterward, mice
180 were monitored for clinical signs and body weight changes. Mice were sacrificed when
181 exhibiting 20% or greater weight loss or severe clinical signs, or at the end of the study to sample
182 spleen and brain from mice.
183 **Infectious virus titration**

184 To quantify infectious loads in DENV, JEV and WNV stocks, the endpoint dilution assay was used
185 to determine the 50% tissue culture infectious dose ($TCID_{50}$), with two replicates, as we had
186 described before [4,15-19]. Viral stocks were serially diluted in four replicates in media and 50 µl
187 of each dilution was added to confluent VERO-ZAP-WT or VERO-ZAP-KO cells cultured in 96-
188 well plates. Dilutions were made in DMEM media with 1% FBS. After 2 h at 37°C, 150 µl of
189 media was added. The cells were incubated for 5-7 days (5 days for WNV; 7 days for DENV and
190 JEV) at 37°C, 5% CO_2. Afterward, plates were washed, dried, formalin fixed, and stained with
191 specific antibodies (Ab) [4,15-19]. For DENV and WNV IHC, we used primary anti-pan flavivirus
192 envelop (E) protein monoclonal Ab D1-4G2-4-15 (ATCC, VA, USA; #HB-112) followed by Goat
193 anti-Mouse IgG HRP Ab (Abcam, MA, USA; #ab97023). For JEV, we used JEV E polyclonal Ab
194 (GeneTex, CA, USA; #GTX125867;) followed by Goat Anti-Rabbit IgG H&L (HRP) Ab (Abcam,
195 MA, USA; #ab97051) [4,15-19]. Infectious titers were calculated by the Spearman-Kärber formula
196 and expressed in $\log_{10}$ $TCID_{50}$ per ml. Media from mock-inoculated cells were used as negative
197 controls.
198

199 **RNA extraction and virus-specific reverse transcriptase quantitative polymerase chain**
200 **reaction assays (RT-qPCR)**

201 The RNA from cell culture supernatants was extracted with QIAamp Viral RNA Mini Kit
202 (QIAGEN) according to the manufacturer's instructions. The RNA from mouse tissues was
203 extracted with PureLink RNA Mini Kit (Invitrogen) according to the manufacturer's instructions.
204 All RT-qPCR reactions were conducted on the QuantStudio 3 real-time PCR system (Applied
205 Biosystems) and analyzed using QuantStudio Design & Analysis Software v1.5.2.

206 For DENV (F: 5′-AAGGACTAGAGGTTAKAGGAGACCC-3′; R: 5′-
207 GGCGYTCTGTGCCTGGAWTGATG-3′; Probe: 56-JOEN/AA CAG CAT A/ZEN/T TGA CGC
208 TGG GAA AGA CC-3IABkFQ), JEV-WT and JEV-CpG (F: 5′-GCCACCCAGGAGGTCCTT-
209 3′; R: 5′-CCCCAAAACCGCAGGAAT-3′; Probe: 56-FAM-CAAGAGGTG/ZEN/GACGGCC-
210 3IABkFQ), and WNV-WT and WNV-Per (F: 5′-AGTAGTTCGCCTGTGTGAGC-3′; R: 5′-
211 GCCCTCCTGGTTTCTTAGA-3′; Probe: FAM-
212 AATCCTCACAAACACTACTAAGTTTGTCA-TAMRA) we used the previously validated
213 probe-based one-step RT-qPCR assays [20-22]. The Luna Universal Probe One-Step RT-qPCR
214 Kit (NEB) reaction mixture (20 µL) consisted of 10 µL Luna Universal Probe One-Step Reaction
215 Mix, 1 µL Luna WarmStart RT Enzyme Mix, 1 µL (10 µM) of forward and reverse primers, 0.5
216 µL of the probe, 2.5 µL nuclease-free water and 4 µL of RNA template. The reverse transcription
217 and enzyme activation steps of 10 min at 55˚C and 1 min at 95˚C were followed by 40
218 amplification cycles (10 s at 95˚C and 30 s at 60˚C). A standard curve was used to quantify viral
219 RNA loads as we described [15].
220
221
222 PCR values were corrected for fluid volumes or tissue weights and upon logarithmical
223 transformation expressed as virus RNA genome copies per ml or g. Strict precautions were taken
224 to prevent PCR contamination. All master mix preparations were done in the dedicated PCR
225 cabinet. Aerosol-resistant filter pipette tips and disposable gloves were used. Kit reagent controls
226 were included in every RNA extraction and PCR run.
227
228

229 **Statistics**

230 We used GraphPad 9 PRISM for statistics. For the comparison of the viral RNA loads, infectious
231 titers, and quantitative IHC we used an unpaired t-test. P-value < 0.05 was considered statistically
232 significant.

233

234 **REFERENCES**

235 1. Nguyen Phuong Khanh Le, Prince Pal Singh, Ahmad Jawad Sabir, Ivan Trus, Uladzimir Karniychuk.
236 Endogenous ZAP is associated with altered global cellular gene expression during Zika virus
237 infection. bioRxiv. 2024.
238 2. Sabir AJ, Le NPK, Singh PP, et al. Endogenous ZAP affects Zika virus RNA interactome. RNA Biol.
239 2024 Jan;21(1):1-10.
240 3. Simmonds P. SSE: a nucleotide and amino acid sequence analysis platform. BMC research notes:
241 BioMed Central; 2012. p. 50.
242 4. Trus I, Udenze D, Berube N, et al. CpG-Recoding in Zika Virus Genome Causes Host-Age-
243 Dependent Attenuation of Infection With Protection Against Lethal Heterologous Challenge in
244 Mice. Front Immunol. 2019;10:3077.
245 5. Trus I, Udenze D, Karniychuk U. Generation of CpG-Recoded Zika Virus Vaccine Candidates.
246 Methods in molecular biology (Clifton, N.J.): Methods Mol Biol; 2022. p. 289-302.
247 6. Gaunt E, Wise HM, Zhang H, et al. Elevation of CpG frequencies in influenza A genome
248 attenuates pathogenicity but enhances host response to infection. eLife2016. p. e12735.
249 7. Atkinson NJ, Witteveldt J, Evans DJ, et al. The influence of CpG and UpA dinucleotide frequencies
250 on RNA virus replication and characterization of the innate cellular pathways underlying virus
251 attenuation and enhanced replication. Nucleic acids research2014. p. 4527-45.
252 8. Tulloch F, Atkinson NJ, Evans DJ, et al. RNA virus attenuation by codon pair deoptimisation is an
253 artefact of increases in CpG/UpA dinucleotide frequencies. eLife2014. p. 1-15.
254 9. Park CJ, Lee YA, Yoo SM, et al. Efficient reverse genetics approach involving infectious
255 subgenomic amplicon for engineering dengue virus. J Med Virol. 2023 Aug;95(8):e28978.
256 10. Aubry F, Nougairede A, Gould EA, et al. Flavivirus reverse genetic systems, construction
257 techniques and applications: a historical perspective. Antiviral Res. 2015 Feb;114:67-85.
258 11. Liu J, Jing W, Fang Y, et al. The Infection of the Japanese Encephalitis Virus SA14-14-2 Strain
259 Induces Lethal Peripheral Inflammatory Responses in IFNAR Deficiency Mice. Frontiers in
260 microbiology: Front Microbiol; 2022.
261 12. Zhang YN, Li N, Zhang QY, et al. Rational design of West Nile virus vaccine through large
262 replacement of 3' UTR with internal poly(A). EMBO Mol Med. 2021 Sep 7;13(9):e14108.
263 13. Daffis S, Samuel MA, Keller BC, et al. Cell-specific IRF-3 responses protect against West Nile virus
264 infection by interferon-dependent and -independent mechanisms. PLoS Pathog. 2007 Jul
265 27;3(7):e106.
266 14. Daffis S, Samuel MA, Suthar MS, et al. Interferon regulatory factor IRF-7 induces the antiviral
267 alpha interferon response and protects against lethal West Nile virus infection. J Virol. 2008
268 Sep;82(17):8465-75.

269 15. Chapagain S, Pal Singh P, Le K, et al. Japanese encephalitis virus persists in the human
270 reproductive epithelium and porcine reproductive tissues. PLoS Negl Trop Dis. 2022
271 Jul;16(7):e0010656.
272 16. Sabir AJ, Singh PP, Trus I, et al. Asian Zika virus can acquire generic African-lineage mutations
273 during in utero infection. Emerg Microbes Infect. 2023 Dec;12(2):2263592.
274 17. Darbellay J, Lai K, Babiuk S, et al. Neonatal pigs are susceptible to experimental Zika virus
275 infection. Emerg Microbes Infect. 2017 Feb 15;6(2):e6.
276 18. Darbellay J, Cox B, Lai K, et al. Zika Virus Causes Persistent Infection in Porcine Conceptuses and
277 may Impair Health in Offspring. EBioMedicine. 25:73-86.2017.
278 19. Trus I, Udenze D, Cox B, et al. Subclinical in utero Zika virus infection is associated with interferon
279 alpha sequelae and sex-specific molecular brain pathology in asymptomatic porcine offspring. In:
280 Pierson TC, editor. PLoS Pathogens2019. p. e1008038.
281 20. Eiden M, Vina-Rodriguez A, Hoffmann B, et al. Two new real-time quantitative reverse
282 transcription polymerase chain reaction assays with unique target sites for the specific and
283 sensitive detection of lineages 1 and 2 West Nile virus strains. J Vet Diagn Invest. 2010
284 Sep;22(5):748-53.
285 21. Shao N, Li F, Nie K, et al. TaqMan Real-time RT-PCR Assay for Detecting and Differentiating
286 Japanese Encephalitis Virus. Biomedical and environmental sciences : BES: Biomed Environ Sci;
287 2018. p. 208-214.
288 22. Callahan JD, Wu SJ, Dion-Schultz A, et al. Development and evaluation of serotype- and group-
289 specific fluorogenic reverse transcriptase PCR (TaqMan) assays for dengue virus. J Clin Microbiol.
290 2001 Nov;39(11):4119-24.

291